Supporting Information

Quasi-isostructural Order-disorder Phase Transitions and Anisotropic Thermal Expansions in Polymorphic Crystals of a Biologically Active Molecule with Distinct Solubility and Dissolution Rate

*Aditya Verma[§], Sourabh[§], Anil Kumar[§], Parthapratim Munshi[§]**

[§]Multifunctional Molecular Materials Laboratory, Department of Chemistry, School of Natural Sciences, Shiv Nadar Institution of Eminence Deemed to be University, NH-91, Tehsil Dadri, Gautam Buddha Nagar, Uttar Pradesh-201314, India.

E-mail: parthapratim.munshi@snu.edu.in

Synthesis and Characterization

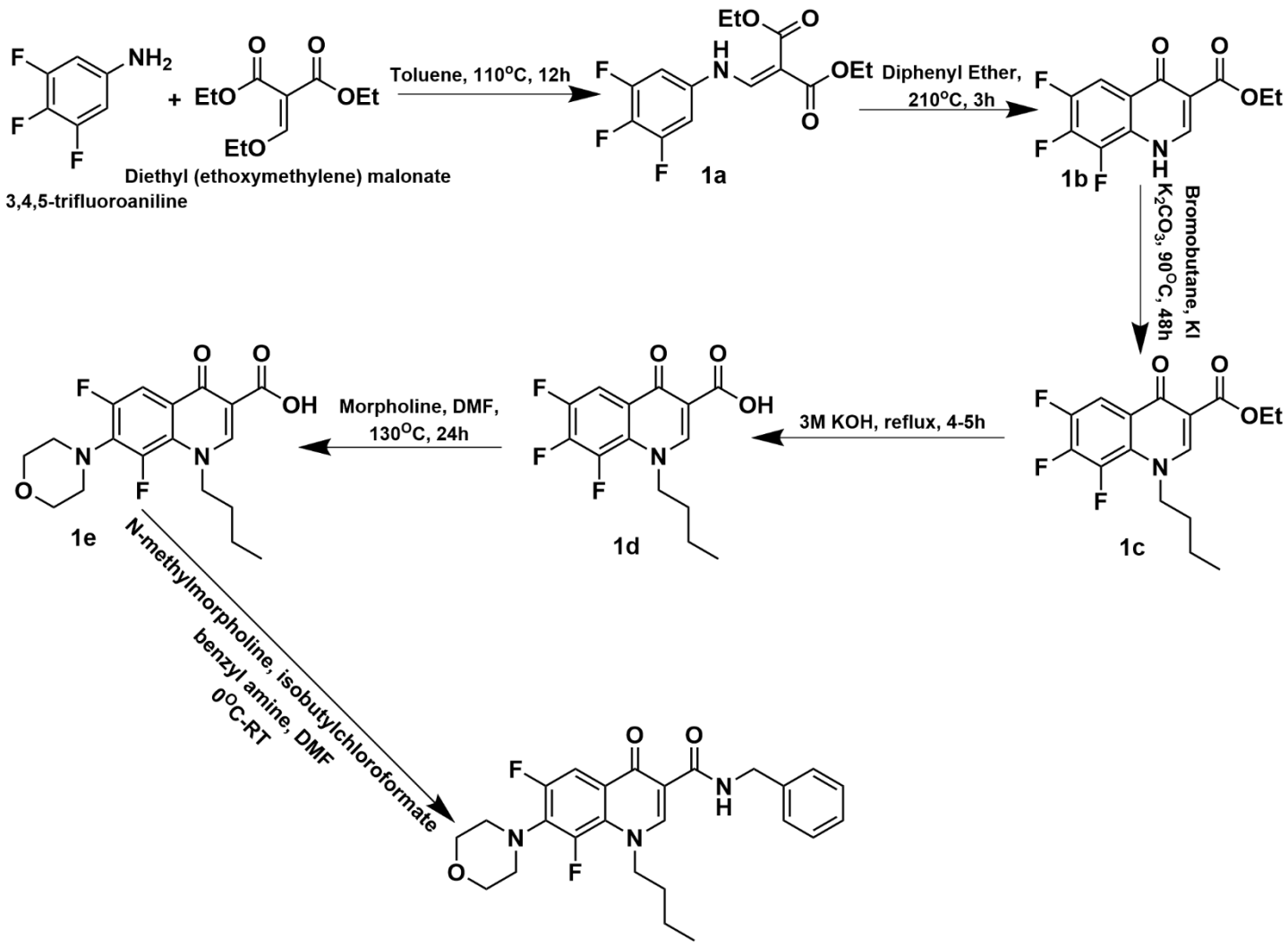

Scheme S1: Reaction scheme of **1**.

Following a previously reported scheme in the literature, the title compound N-benzyl-1-butyl-6,8-difluoro-7-morpholino-4-oxo-1,2,3,4-tetrahydroquinoline-3-carboxamide (**1**) has been synthesized. 1 equivalent of the starting compound, 3,4,5-trifluoroaniline was dissolved in 3 ml of diethyl (ethoxymethylene) malonate in a 100 ml round bottom flask and stirred for 12 hours at 110ºC upon addition of toluene. The product **1a** was isolated via column chromatography. This was then reacted with diphenyl ether at 210ºC for 3 hours to obtain **1b**, which was isolated by filtration of the reaction mixture and dried completely. The subsequent reaction of **1b** with 5 equivalents of bromobutane, 5 equivalents of potassium carbonate and DMF as a solvent, and subsequent isolation via column chromatography gave **1c**. This product was refluxed with 5M KOH for 4-5 hours to give **1d**. An addition of 0.5 ml of morpholine and 10 ml of DMF and stirring at 130ºC for 24 hours gave product **1e**, which was isolated by column chromatography. The final step involved treating **1e** with 1 equivalent of N-methyl

morpholine, 4 equivalents of isobutyl chloroformate and 4 equivalents of benzyl amine. The resulting mixture was purified via column chromatography and subsequent recrystallization gave the final compound **1**, with a yield of 30%.

The formation of the product was confirmed by characterization via ^{1}H and ^{13}C NMR figures in **S1(a)** and **S1(b)** and high-resolution electrospray ionization mass spectrometry (HR-ESIMS) figure in **S1(c)**.

^{1}H NMR (400 MHz; $CDCl_3$): δ_H 10.26 (t; 1H), 8.64 (s, 1H), 7.97 (dd, 1H), 7.39 (m, 5H), 7.24 (m, 1H), 4.62 (d, 2H), 4.48 (m, 3H), 3.85 (m, 4H), 3.3 (s, 4H), 1.87 (p, 2H), 1.45 (sext, 2H), 0.99 (t, 3H). ^{13}C NMR (100 MHz, $CDCl_3$): δ 165.1 (s), 150.4 (s), 139.2 (s), 129.1 (s), 128.1 (s), 127.9 (s), 127.8 (s), 127.6 (s), 111.3 (s), 109.1 (s), 108.8 (d), 67.9 (s), 59.2 (s), 59.0 (s), 51.8 (s), 45.1 (s), 43.8 (s), 33.3 (s), 20.2 (s), 14.1 (s).

HR-ESIMS (m/z): calculated for $C_{25}H_{27}N_3O_3F_2$ $[M+H]^+$: 456.2093; found $C_{25}H_{27}N_3O_3F_2$ $[M+H]^+$: 456.2117.

(a) ^{1}H NMR

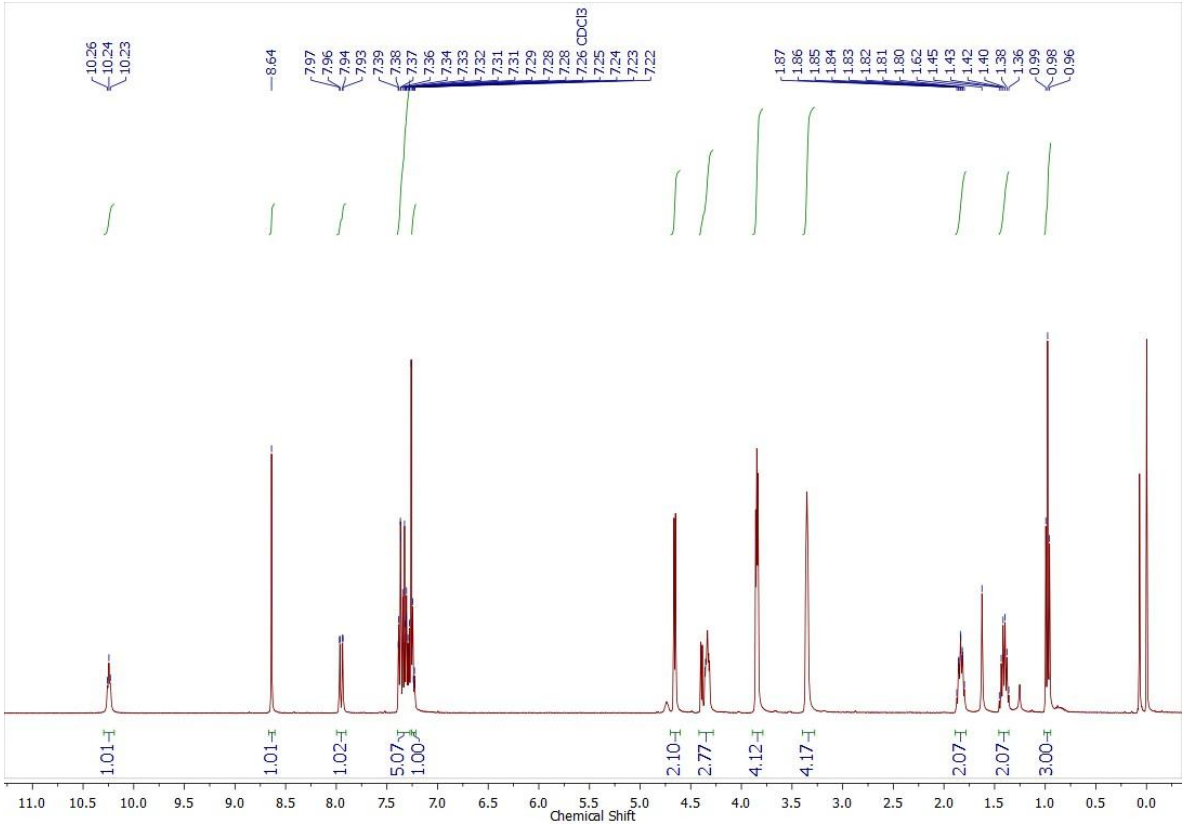

(b) ^{13}C NMR

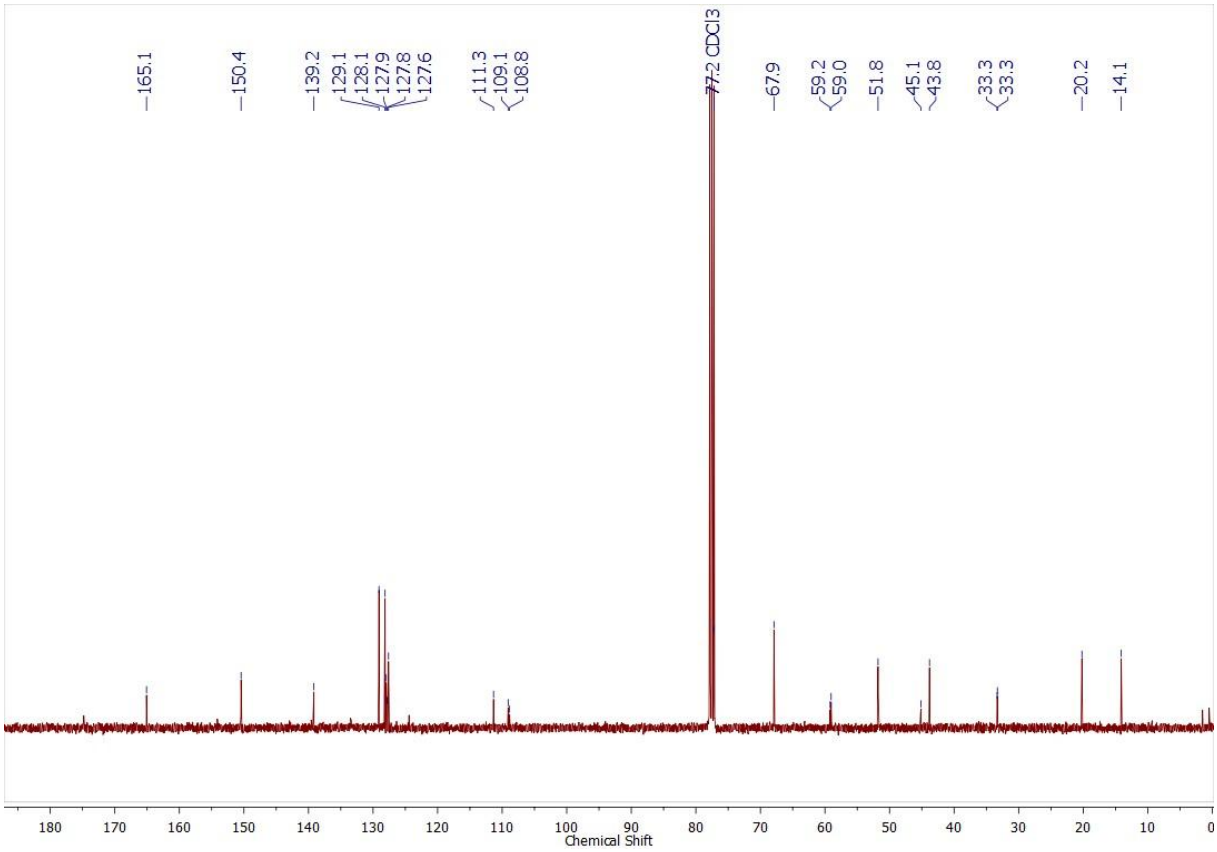

(c) HR-ESIMS

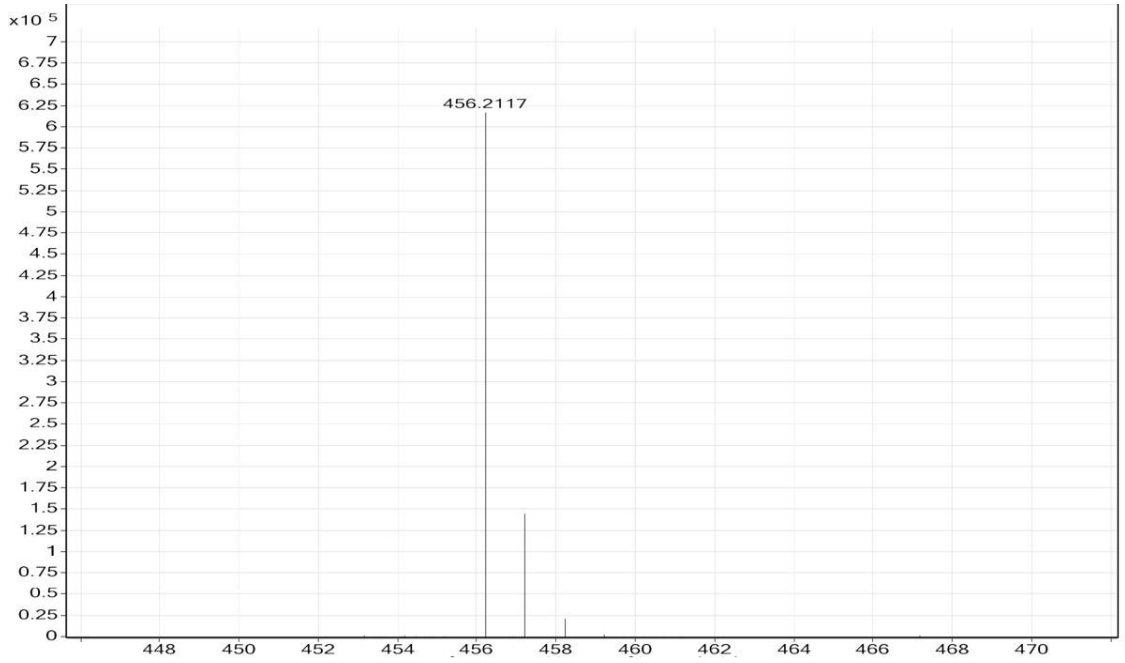

Figure S1: **(a)** ^{1}H NMR, **(b)** ^{13}C NMR, and **(c)** HR-ESIMS of **1**.

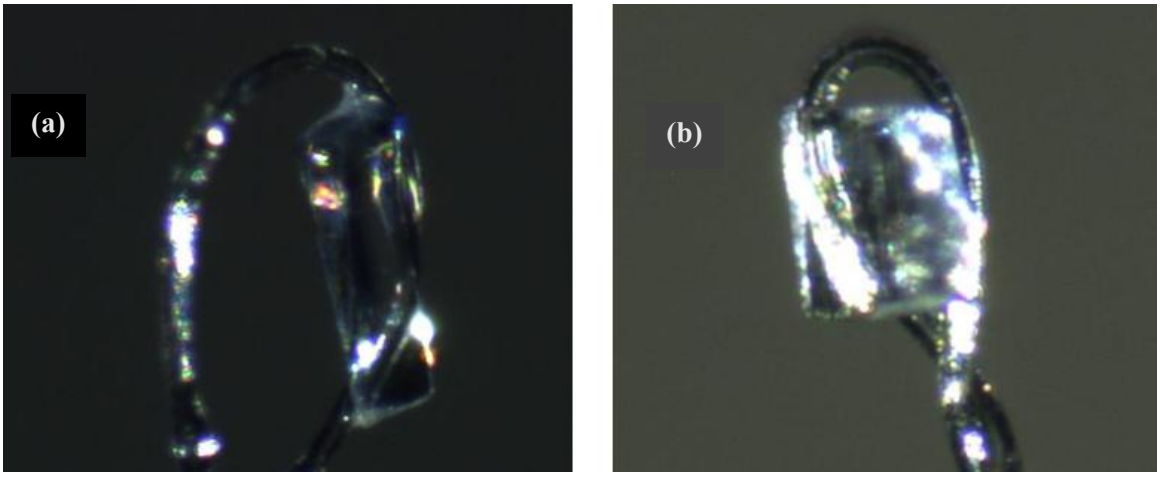

Figure S2: Block-shaped single crystals of **(a) Form I** and **(b) Form II**.

Table S1: Crystallization details using the vapor diffusion method in various solvents in the 1:1 ratio. RT and LT refer to Room (25ºC) and Low (4ºC) Temperature, respectively.

Inner Solvent	Diffusion Solvent	Condition	Morphology
Ethanol	Acetone	LT	Needle
Methanol	Acetone	LT	Needle
Ethyl Acetate	Hexane	LT	Block
Ethyl Acetate	Dichloromethane	LT	Needle
Benzene	Acetone	LT	--

Table S2: Crystallization details using the slow evaporation method in various solvents.

Solvent	Condition	Morphology
Dimethyl Formamide (DMF)	RT	Needle
Ethanol	RT	Block
Methanol	RT	Block
Acetone	RT	Block
Ethanol	LT	Needle
Methanol	LT	Block
Acetonitrile	RT	Needle/Block
1,4-Dioxane	RT	Block
Toluene	RT	Needle
Isopropanol	RT	--
Isobutanol	RT	--
Ethyl Acetate	LT	Needle
Benzene	RT	Needle
p-Xylene	RT	Needle
o-Xylene	RT	--

Table S3: Crystal data and refinement parameters at variable temperatures of **Form I**.

Temperature	**298K**	**225K**	**210K**	**160K**	**150K**	**140K**	**130K**	**120K**	**100K**
CCDC #	2386813	2386814	2386810	2386809	2386811	2386815	2386816	2386812	2386889
Chemical Formula	$C_{25}H_{27}N_3O_3F_2$								
Formula Weight (g/mol)	455.49								
a (Å)	5.4526(2)	5.3871(4)	5.3763(2)	**5.3504(1)**	**10.6998(3)**	10.6853(2)	10.6773(2)	10.6690(2)	10.6475(4)
b (Å)	13.8271(5)	13.7306(11)	13.7145(5)	13.6627(4)	13.7430(4)	13.7323(3)	13.7320(4)	13.7277(3)	13.7206(4)
c (Å)	15.4128(6)	15.4560(12)	15.4507(6)	15.4350(4)	15.4384(4)	15.4315(4)	15.4286(4)	15.4240(4)	15.4089(4)
α (º)	94.769(1)	94.989(3)	94.997(1)	**95.021(1)**	**84.140(1)**	84.129(1)	84.138(1)	84.132(1)	84.132(1)
β (º)	92.424(1)	92.216(3)	92.174(1)	**92.042(1)**	**88.165(1)**	88.230(1)	88.267(1)	88.288(1)	88.421(1)
γ (º)	101.093(1)	100.770(3)	100.706(1)	**100.403(1)**	**77.559(1)**	77.424(1)	77.324(1)	77.217(1)	77.071(1)
Volume, *V* (Å³)	1134.35(7)	1117.10(15)	1113.44(7)	**1103.98(5)**	**2205.17(11)**	2198.32(9)	2195.40(10)	2191.42(9)	2182.50(12)
Space Group	$P\bar{1}$								
Z; Z'	2; 1				4; 2				
R(*F*); $R_w(F)$	0.0509; 0.1015	0.0569; 0.1349	0.0551; 0.1231	0.0587; 0.1292	0.0863; 0.2913	0.0580; 0.1850	0.0722; 0.2395	0.0667; 0.2107	0.0361; 0.1042
GooF (S)	1.041	1.093	1.016	1.017	1.11	1.089	1.099	1.106	1.027
Peak; Hole (e/Å³)	0.3; -0.2	0.3; -0.2	0.2; -0.2	0.3; -0.3	0.5; -0.4	0.3; -0.3	0.4; -0.4	0.3; -0.4	0.3; -0.2

Table S4: Crystal data and refinement parameters at variable temperatures of **Form II.**

Temperature	**298K**	**225K**	**210K**	**170K**	**150K**	**140K**	**130K**	**120K**	**100K**
CCDC #	2386802	2386807	2386805	2386804	2386803	2386808	2386806	2386801	2386800
Chemical Formula	$C_{25}H_{27}N_3O_3F_2$								
Formula Weight (g/mol)	455.49								
a (Å)	6.0713(2)	6.0544(2)	**6.0472(2)**	**12.2289(3)**	12.2135(8)	12.2144(7)	12.2086(3)	12.2041(3)	12.1961(3)
b (Å)	15.0980(5)	15.1710(4)	15.1916(11)	14.6129(4)	14.5839(11)	14.5808(10)	14.5790(4)	14.5742(3)	14.5683(3)
c (Å)	24.9433(8)	24.6379(7)	24.5820(17)	24.8725(7)	24.8400(17)	24.8197(16)	24.8022(7)	24.7844(5)	24.7525(5)
α (º)	90.000	90.000	90.000	90.000	90.000	90.000	90.000	90.000	90.000
β (º)	94.423(1)	95.147(1)	95.256(2)	93.983(1)	93.988(3)	94.020(2)	94.064(1)	94.094(1)	94.146(1)
γ (º)	90.000	90.000	90.000	90.000	90.000	90.000	90.000	90.000	90.000
Volume, *V* (Å³)	2279.61(13)	2253.90(11)	**2248.80(3)**	**4434.50(2)**	4413.8(5)	4409.4(5)	4403.4(2)	4397.43(17)	4386.43(18)
Space Group	$P2_1/c$								
Z; Z'	**4; 1**			**8; 2**					
R(*F*); $R_w(F)$	0.0689; 0.2268	0.0614; 0.1925	0.0623; 0.1834	0.0668; 0.2423	0.0703; 0.2566	0.0612; 0.2152	0.0547; 0.1827	0.0550; 0.1785	0.0583; 0.1954
GooF (S)	1.079	1.075	1.052	1.050	1.068	1.080	1.060	1.072	1.090
Peak; Hole (e/Å³)	0.5; -0.6	0.5; -0.3	0.3; -0.2	0.3; -0.3	1.1; -0.3	0.8; -0.3	0.7; -0.3	0.7; -0.3	0.7; -0.3

Table S5: Crystal data and refinement parameters at variable temperatures of **Form I**.

Temperature	**298K**	**150K**		**140K**		**130K**		**120K**		**100K**	
Space Group	*P*-1	*P*-1									
Z; Z'	2; 1	2; 1									
Model	Without *q*-vector	Without *q*-vector	With *q*-vector*	Without *q*-vector	With *q*-vector*	Without *q*-vector	With *q*-vector*	Without *q*-vector	With *q*-vector*	Without *q*-vector	With *q*-vector*
a (Å)	5.4526(2)	10.6998(3)	5.3517(1)	10.6853(2)	5.3459(1)	10.6773(2)	5.3416(10)	10.6690(2)	5.3384(9)	10.6475(4)	5.3247(8)
b (Å)	13.8271(5)	13.7430(4)	13.6383(3)	13.7323(3)	13.6235(25)	13.7320(4)	13.6120(29)	13.7277(3)	13.6019(26)	13.7206(4)	13.5632(20)
c (Å)	15.4128(6)	15.4384(4)	15.4438(3)	15.4315(4)	15.4468(29)	15.4286(4)	15.4415(32)	15.4240(4)	15.4418(30)	15.4089(4)	15.4115(23)
α (°)	94.769(1)	84.140(1)	95.1940(7)	84.129(1)	95.229(7)	84.138(1)	95.242(8)	84.132(1)	95.260(7)	84.132(1)	95.314(5)
β (°)	92.424(1)	88.165(1)	91.8210(8)	88.230(1)	91.7791(7)	88.267(1)	91.740(7)	88.288(1)	91.7278(7)	88.421(1)	91.578(6)
γ (°)	101.093(1)	77.559(1)	100.0905(7)	77.424(1)	99.9482(6)	77.324(1)	99.843(7)	77.217(1)	99.7282(6)	77.071(1)	99.573(5)
Volume, *V* (Å^3)	1134.35(7)	2205.17(11)	1103.91(6)	2198.32(9)	1102.20(5)	2195.40(10)	1100.39(6)	2191.42(9)	1099.31(5)	2182.50(12)	1091.77(4)
R(*F*); R_w(*F*)	0.0509; 0.1015	**0.0863; 0.2913**	**0.0951; 0.2189**	**0.0580; 0.1850**	**0.0862; 0.1997**	**0.0722; 0.2395**	**0.1027; 0.2219**	**0.0667; 0.2107**	**0.0991; 0.2251**	**0.0361; 0.1042**	**0.0814; 0.1821**
GooF (S)	1.041	**1.11**	**3.91**	**1.08**	**3.96**	**1.09**	**3.86**	**1.10**	**4.54**	**1.02**	**4.05**
Peak; Hole (e/Å^3)	0.3; -0.2	0.5; -0.4	0.6; -0.4	**0.3; -0.3**	**0.8; -1.0**	**0.4; -0.4**	**0.9; -0.8**	**0.3; -0.4**	**0.9; -1.0**	**0.3; -0.2**	**1.0; -1.3**
Q-vectors **(0.5, 0.5, 0)**			0.49999(3)		0.49996(3)		0.50001(3)		0.49989(3)		0.50019(2)
			0.49983(8)		0.50009(7)		0.49981(7)		0.50033(7)		0.49994(5)
			-0.00006(9)		-0.00007(8)		-0.00014(8)		0.00022(8)		0.00014(6)

***** Refined using JANA2020 (*Z. Kristallogr*. 238(7–8) (2023) 271 – 282).

Table S6: Crystal data and refinement parameters at variable temperatures of **Form II**.

Temperature	**298K**	**100K**	
Space Group	$P2_1/c$	$P2_1/c$	
Z; Z'	4; 1	4; 1	
Model	Without *q*-vector	Without *q*-vector	With *q*-vector*
a (Å)	6.0713(2)	12.1961(3)	6.1021(1)
b (Å)	15.0980(5)	14.5683(3)	14.5785(2)
c (Å)	24.9433(8)	24.7525(5)	24.7684(4)
β (°)	94.423(1)	94.146(1)	94.1299(6)
Volume, *V* (Å^3)	2279.61(13)	4386.43(18)	2197.65(9)
R(*F*); R_w(*F*)	0.0689; 0.2268	**0.0583; 0.1954**	**0.0894; 0.2085**
GooF (S)	1.079	**1.090**	**4.8627**
Peak; Hole (e/Å^3)	0.5; -0.6	**0.7; -0.3**	**0.5; -0.9**
Q-vectors **(0.5, 0, 0)**			0.50001(3)
			0.00002(7)
			0.00006(12)

Table S7: Determination of unit cell parameters at variable temperatures, 298K to 100K, of **Form I**.

Temperature (K)	*a* (Å)	*b* (Å)	*c* (Å)	α (°)	β (°)	γ (°)	*V* (Å^3)
298	5.4380(5)	13.8228(13)	15.3952(12)	94.8824(41)	92.4819(29)	101.0475(44)	1129.560(26)
280	5.4314(2)	13.7894(5)	15.4249(5)	94.7821(17)	92.3603(11)	100.9820(16)	1128.235(10)
260	5.4129(15)	13.7595(42)	15.4335(40)	94.8865(15)	92.3335(8)	100.8533(14)	1122.914(9)
240	5.3933(17)	13.7350(45)	15.4283(46)	94.9586(16)	92.2493(11)	100.7658(16)	1116.770(10)
220	5.3822(17)	13.7111(47)	15.4476(46)	94.9684(17)	92.2342(10)	100.7472(15)	1114.000(10)
200	5.3705(16)	13.7002(44)	15.4410(45)	94.9843(15)	92.1784(10)	100.6584(13)	1110.578(10)
180	5.3595(13)	13.6820(37)	15.4429(37)	94.9440(14)	92.1348(8)	100.5487(11)	1107.502(8)
160	**5.3442(19)**	**13.6551(57)**	**15.4272(53)**	**94.9792(18)**	**92.0373(11)**	**100.4312(16)**	**1101.514(11)**
150	**10.6931(39)**	**13.7470(63)**	**15.4449(52)**	**84.1516(18)**	**88.2297(12)**	**77.5536(16)**	**2205.362(23)**
140	10.6871(36)	13.7593(55)	15.4416(54)	84.1548(18)	88.2823(12)	77.4233(15)	2204.576(21)
130	10.6847(35)	13.7554(58)	15.4455(48)	84.1140(17)	88.2815(12)	77.2841(14)	2202.660(20)
120	10.6845(32)	13.7713(48)	15.4530(50)	84.1324(18)	88.3082(12)	77.2107(14)	2205.660(18)
110	10.6665(37)	13.7470(49)	15.4334(55)	84.1426(18)	88.3645(11)	77.1342(13)	2194.677(21)
100	10.6669(35)	13.7475(45)	15.4349(50)	84.1753(18)	88.3441(11)	77.0285(12)	2194.235(19)

Table S8: Determination of unit cell parameters at variable temperatures, 100K to 298K, of **Form I**.

Temperature (K)	*a* (Å)	*b* (Å)	*c* (Å)	α (°)	β (°)	γ (°)	*V* (Å^3)
100	10.6620(35)	13.7497(39)	15.4297(55)	84.1670(18)	88.3536(12)	77.0138(13)	2192.679(19)
110	10.6676(41)	13.7482(57)	15.4300(57)	84.1810(19)	88.3474(13)	77.1454(15)	2194.858(23)
120	10.6804(41)	13.7615(55)	15.4463(57)	84.1558(19)	88.3305(13)	77.1918(16)	2202.226(22)
130	10.6705(39)	13.7378(70)	15.4236(61)	84.1350(21)	88.3033(13)	77.2960(18)	2193.990(25)
140	10.6859(41)	13.7502(59)	15.4382(55)	84.1249(18)	88.2688(13)	77.4076(16)	2202.124(23)
150	10.6985(37)	13.7546(54)	15.4500(51)	84.1706(16)	88.2195(11)	77.5412(15)	2208.416(21)
160	**10.6620(35)**	**13.7497(39)**	**15.4297(55)**	**84.2141(16)**	**88.1179(11)**	**77.7643(15)**	**2204.897(23)**
180	**5.3611(17)**	**13.6834(47)**	**15.4487(48)**	**94.9349(15)**	**92.1474(10)**	**100.5445(15)**	**1108.374(10)**
200	5.3709(18)	13.6961(52)	15.4393(49)	94.9161(16)	92.1691(10)	100.7246(15)	1110.102(11)
220	5.3803(16)	13.7064(48)	15.4402(44)	94.9557(17)	92.2217(10)	100.7914(17)	1112.551(9)
240	5.3902(17)	13.7224(49)	15.4292(43)	94.9161(16)	92.2544(10)	100.8241(17)	1115.027(9)
260	5.4071(18)	13.7562(46)	15.4283(46)	94.8651(16)	92.2823(10)	100.8779(15)	1121.068(10)
280	5.4322(19)	13.7935(48)	15.4294(52)	94.7622(18)	92.3668(11)	100.9684(16)	1129.145(11)
298	5.4512(23)	13.8181(58)	15.4261(65)	94.6902(22)	92.4146(14)	101.1022(20)	1134.426(13)

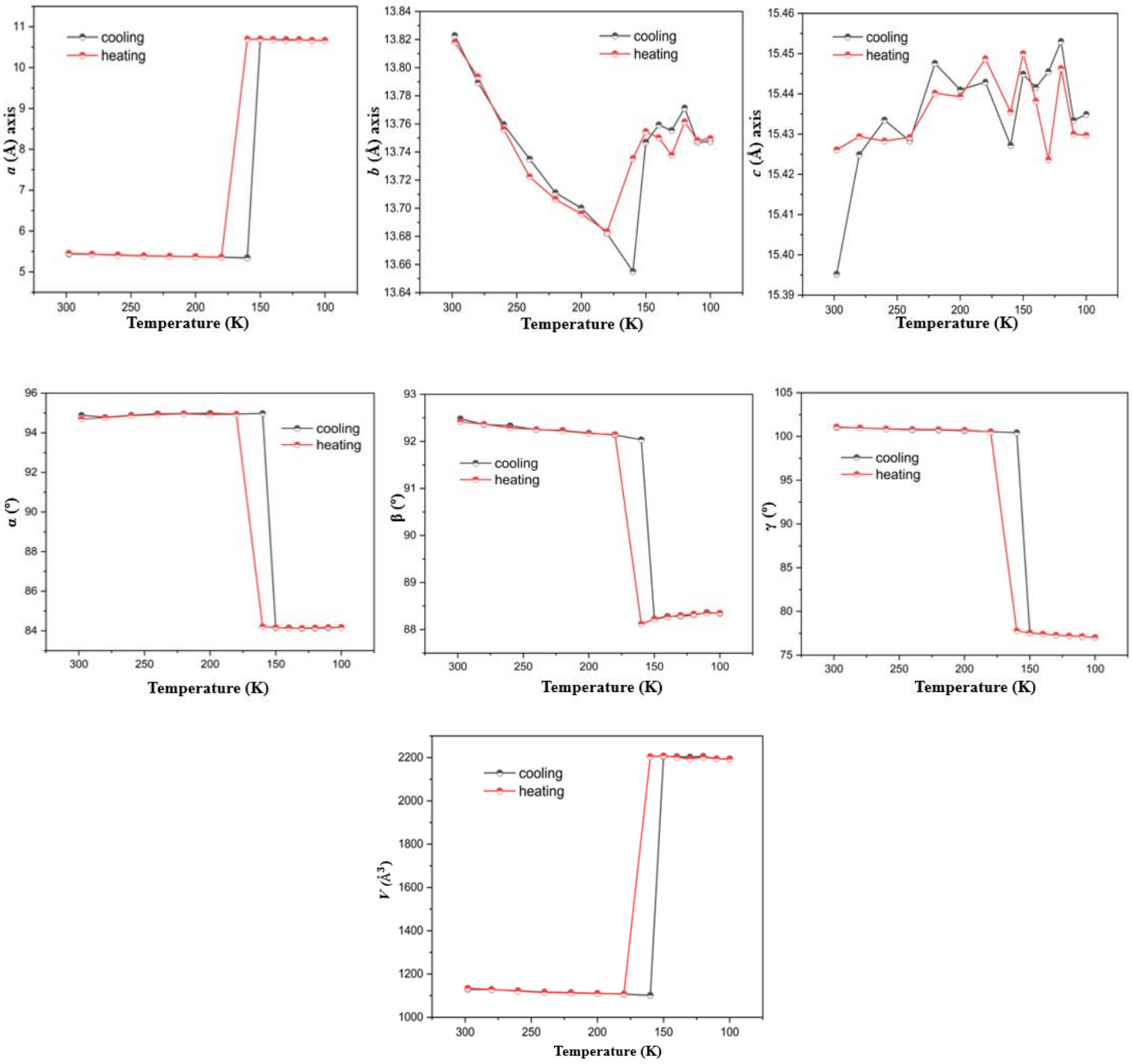

Figure S3: Variation of the unit-cell parameters with respect to temperature of **Form I**.

Table S9: Slopes ($\Delta l/\Delta T$; $\Delta V/\Delta T$) calculated based on the data listed in **Table S7** for **Form I.**

Temperature Range	a ($\times$ 10^{-4}Å/K)	b ($\times$ 10^{-4}Å/K)	c ($\times$ 10^{-4}Å/K)	V(Å^3/K)
298-160K	6.79	12.15	-2.31	0.20
150-100K	5.24	-0.10	2.00	0.22

Table S10: Determination of unit cell parameters at variable temperatures, 298K to 100K, of **Form II**.

Temperature (K)	*a* (Å)	*b* (Å)	*c* (Å)	α (º)	β (º)	γ (º)	*V* (Å^3)
298	6.0799(39)	15.1011(44)	24.9934(83)	90.0000	94.2988(21)	90.0000	2288.280(27)
280	6.0869(19)	15.1613(47)	24.9581(75)	90.0000	94.5024(15)	90.0000	2296.168(20)
260	6.0757(19)	15.1757(49)	24.8455(71)	90.0000	94.7007(14)	90.0000	2283.124(19)
240	6.0686(19)	15.1945(46)	24.7477(69)	90.0000	94.9348(14)	90.0000	2273.492(19)
220	6.0493(12)	15.1893(31)	24.6282(45)	90.0000	95.1472(9)	90.0000	2253.816(12)
200	6.0518(18)	15.2291(37)	24.5717(58)	90.0000	95.3490(12)	90.0000	2254.754(16)
180	**6.0510(16)**	**15.2644(35)**	**24.5306(56)**	**90.0000**	**95.5464(10)**	**90.0000**	**2255.151(15)**
170	**12.2409(33)**	**14.6340(35)**	**24.8764(59)**	**90.0000**	**93.9335(11)**	**90.0000**	**4445.696(30)**
160	12.2372(34)	14.6194(34)	24.8917(61)	90.0000	93.9849(10)	90.0000	4442.379(30)
150	12.2379(31)	14.6229(32)	24.8974(53)	90.0000	93.9796(10)	90.0000	4444.724(27)
140	12.2267(28)	14.6100(31)	24.8634(51)	90.0000	94.0124(10)	90.0000	4430.500(25)
130	12.2264(26)	14.6096(27)	24.8523(46)	90.0000	94.1006(9)	90.0000	4427.833(23)
120	12.2153(28)	14.5945(29)	24.8205(50)	90.0000	94.1136(9)	90.0000	4413.477(25)
110	12.2231(23)	14.6051(26)	24.8297(43)	90.0000	94.1366(8)	90.0000	4421.031(22)
100	12.2153(23)	14.5953(27)	24.8122(44)	90.0000	94.1339(8)	90.0000	4412.178(22)

Table S11: Determination of unit cell parameters at variable temperatures, 100K to 298K, of **Form II**.

Temperature (K)	*a* (Å)	*b* (Å)	*c* (Å)	α (º)	β (º)	γ (º)	*V* (Å^3)
100	12.2153(23)	14.5953(27)	24.8122(44)	90.0000	94.1339(8)	90.0000	4412.178(22)
110	12.2219(24)	14.6077(26)	24.8313(41)	90.0000	94.1348(8)	90.0000	4421.679(21)
120	12.2167(27)	14.5963(31)	24.8215(49)	90.0000	94.1203(9)	90.0000	4414.700(25)
130	12.2214(28)	14.6068(33)	24.8466(54)	90.0000	94.0500(9)	90.0000	4424.439(27)
140	12.2282(50)	14.6174(51)	24.8781(79)	90.0000	94.0292(18)	90.0000	4435.835(42)
150	12.2357(33)	14.6178(35)	24.8861(60)	90.0000	93.9620(11)	90.0000	4440.466(31)
160	12.2301(27)	14.6175(28)	24.8822(45)	90.0000	93.9578(9)	90.0000	4497.691(23)
170	**12.2360(27)**	**14.6316(30)**	**24.8990(50)**	**90.0000**	**93.9177(9)**	**90.0000**	**4447.313(25)**
180	**6.0418(16)**	**15.2479(34)**	**24.5114(56)**	**90.0000**	**95.5638(10)**	**90.0000**	**2247.491(15)**
200	6.0435(17)	15.2155(44)	24.5415(71)	90.0000	95.4240(11)	90.0000	2246.618(18)
220	6.0635(19)	15.2117(37)	24.6599(60)	90.0000	95.1469(12)	90.0000	2265.365(17)
240	6.0750(24)	15.2040(44)	24.7818(73)	90.0000	94.9408(16)	90.0000	2272.696(20)
260	6.0727(26)	15.1591(62)	24.8454(10)	90.0000	94.7220(19)	90.0000	2279.408(26)
280	6.0809(25)	15.1233(53)	24.8848(79)	90.0000	94.5563(14)	90.0000	2281.255(22)
298	6.0799(39)	15.1011(44)	24.9934(83)	90.0000	94.2988(22)	90.0000	2288.280(27)

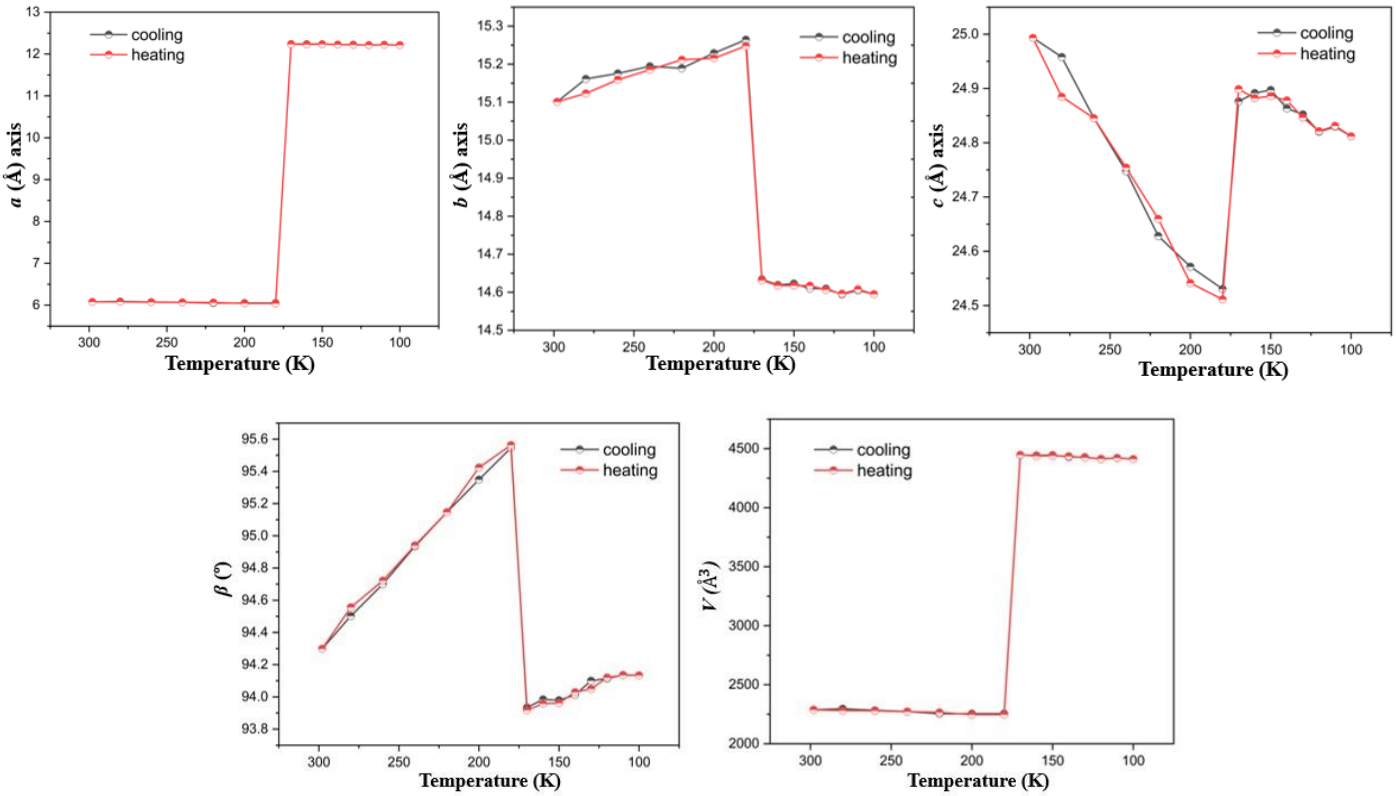

Figure S4: Variation of the unit-cell parameters with respect to temperature of **Form II**.

Table S12: Slopes ($\Delta l/\Delta T$; $\Delta V/\Delta T$) calculated based on the data listed in **Table S10** for **Form II.**

Temperature Range	***a*** $(\times\ \mathbf{10^{-4}}\text{Å}/\boldsymbol{K})$	***b*** $(\times\ \mathbf{10^{-4}}\text{Å}/\boldsymbol{K})$	***c*** $(\times\ \mathbf{10^{-4}}\text{Å}/\boldsymbol{K})$	***V*** $(\text{Å}^3/\boldsymbol{K})$
298-180K	2.44	-13.83	39.22	0.28
170-100K	3.65	5.53	9.17	0.48

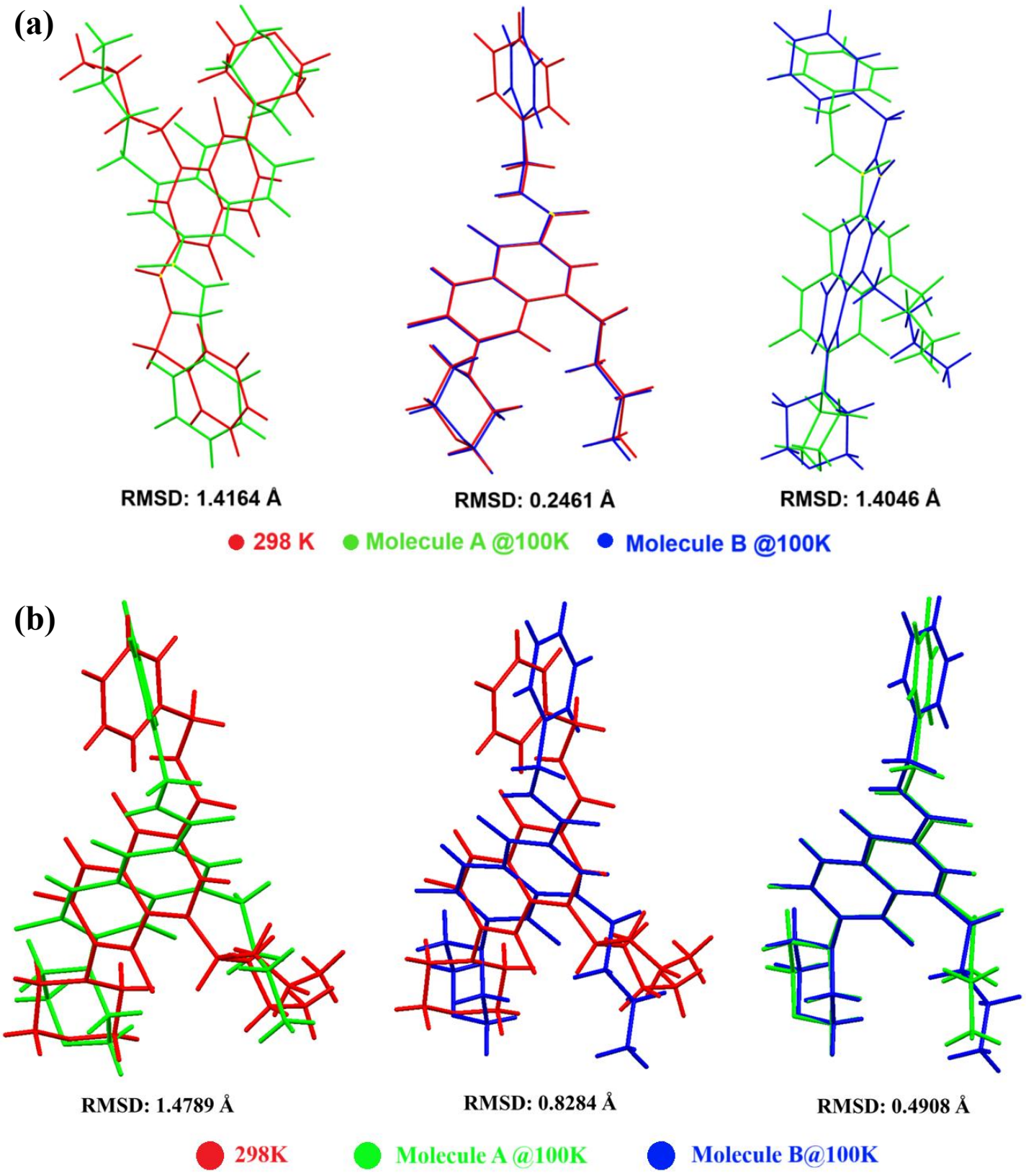

Figure S5: Molecular overlay of the **(a)** molecule of the crystal structure of HT phase with the two crystallographically independent molecules of the crystal structure at LT phase of Form I and (b) molecule of the crystal structure of HT phase with the two crystallographically independent molecules of the structure of LT phase of **Form II**. The molecular overlays between the two molecules of the LT phase of both **Form I** and **Form II** are also shown alongside.

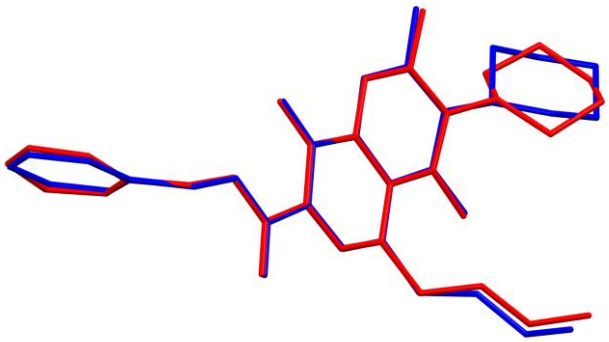

RMSD: 0.284 Å

Figure S6: Molecular overlay of the major conformer of the molecule in **Form I** (in red) and that of **Form II** (in blue). H-atoms omitted for clarity.

Table S13: Selected torsional angles of the HT and LT phases of **Form I** and **Form II**.

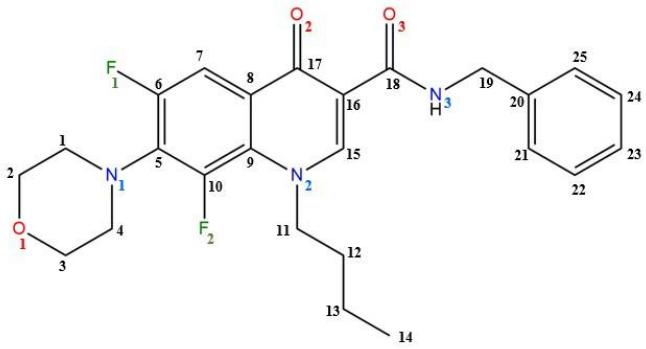

HT Phase Temperatures (K)	**Torsional Angles (º) (C18-N3-C19-C20)**	
	Form I	**Form II**
298	-106.9(2)	-110.0(3)
225	**106.4(2)**	109.5(3)
210	-106.3(2)	109.2(3)
160	-106.3(2)	-

LT phase Temperatures (K)	**Torsional Angles (º) (N3-C19-C20-C25)**		**Torsional Angles (º) (C18-N3-C19-C20)**	
	Form I		**Form II**	
	Molecule A	**Molecule B**	**Molecule A**	**Molecule B**
170	-	-	107.6(3)	104.5(3)#
150	-151.0(3)	112.6(3)	-107.8(3)	-103.8(3)
140	-152.9(3)	111.2(3)	107.6(3)	103.4(3)
130	**-110.0(3)**	**153.6(3)**	-107.8(3)	-103.2(3)
120	-154.2(3)	107.6(3)	-107.7(3)	-103.2(3)
100	-155.3(3)	108.7(3)	107.6(3)	103.1(2)

#Based on the major conformer

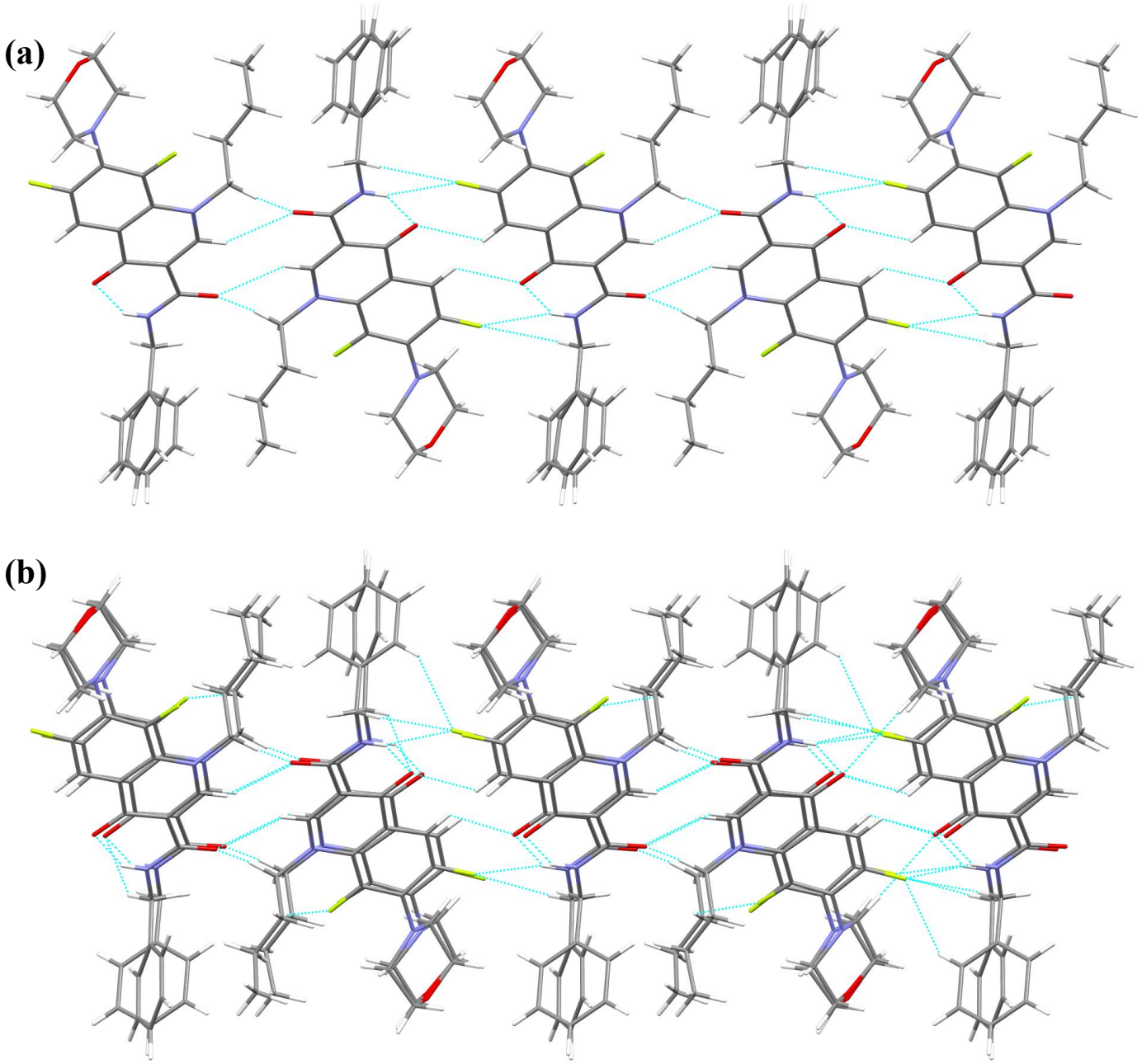

Figure S7: Intra- and intermolecular hydrogen bonds viewed down the *a*-axis in **(a) HT** (major conformer, *Z'* = 1) and **(b) LT** (*Z'* = 2) structures of **Form I**.

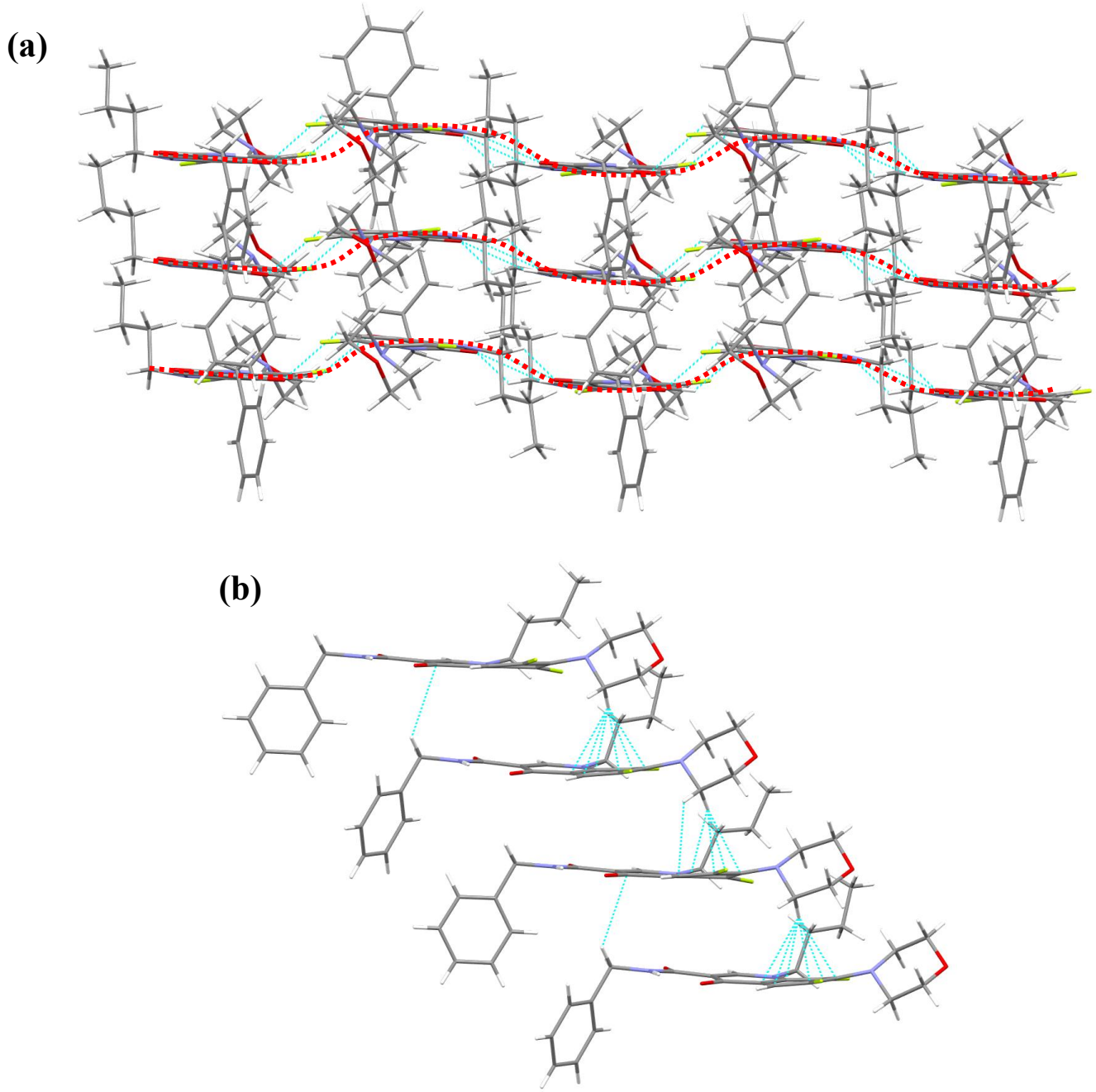

Figure S8: (a) highlighting the ripple-like layered structure and **(b)** stacking of layers via $C-H\cdots\pi$ interactions in the **LT** structure of **Form I**. The **HT** structure displays a similar packing.

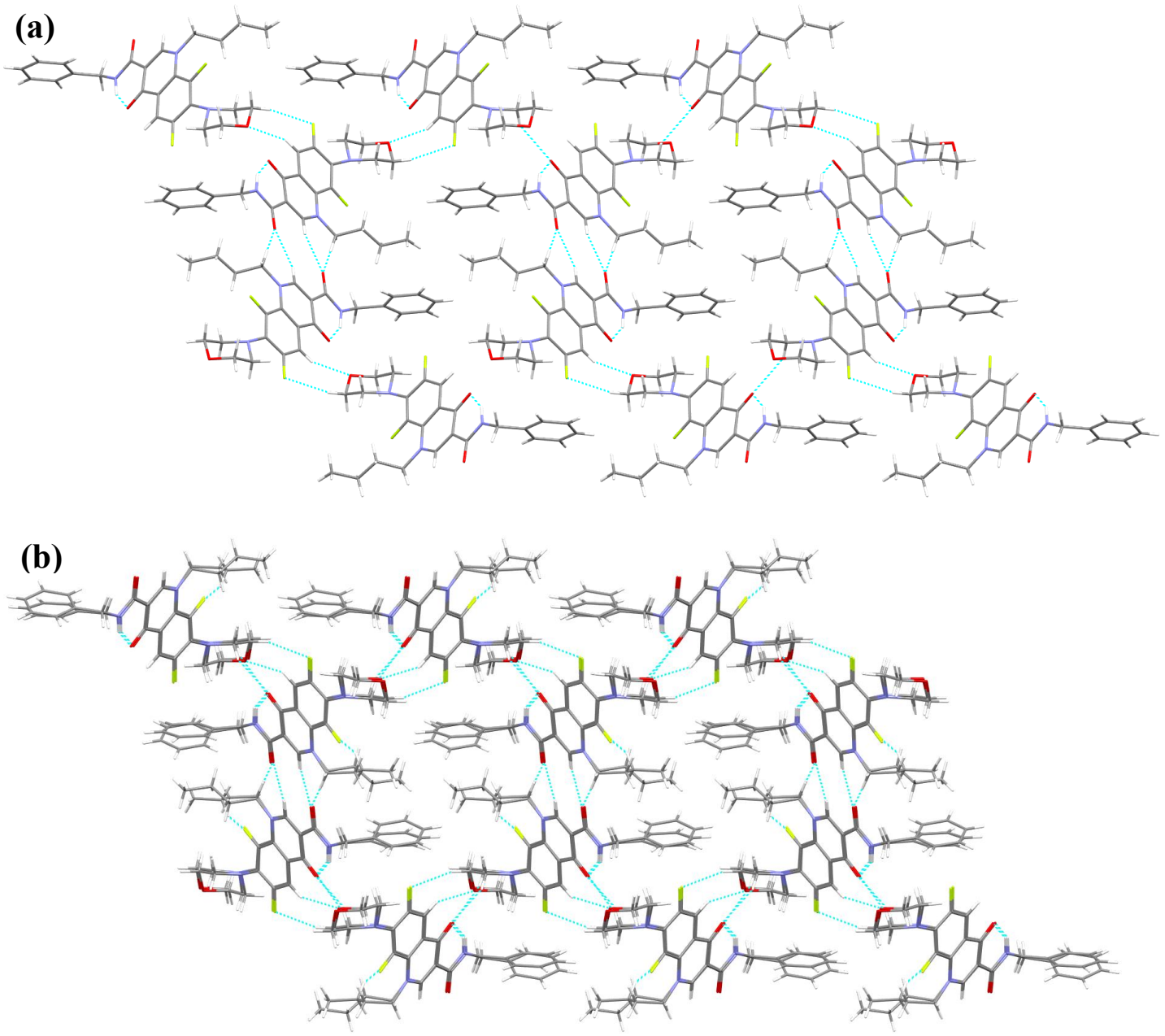

Figure S9: Inter- and intramolecular hydrogen bonds viewed down the *a*-axis in **(a) HT** (major conformer, *Z'*=1)) and **(b) LT** structures (*Z'*=2) of **Form II**.

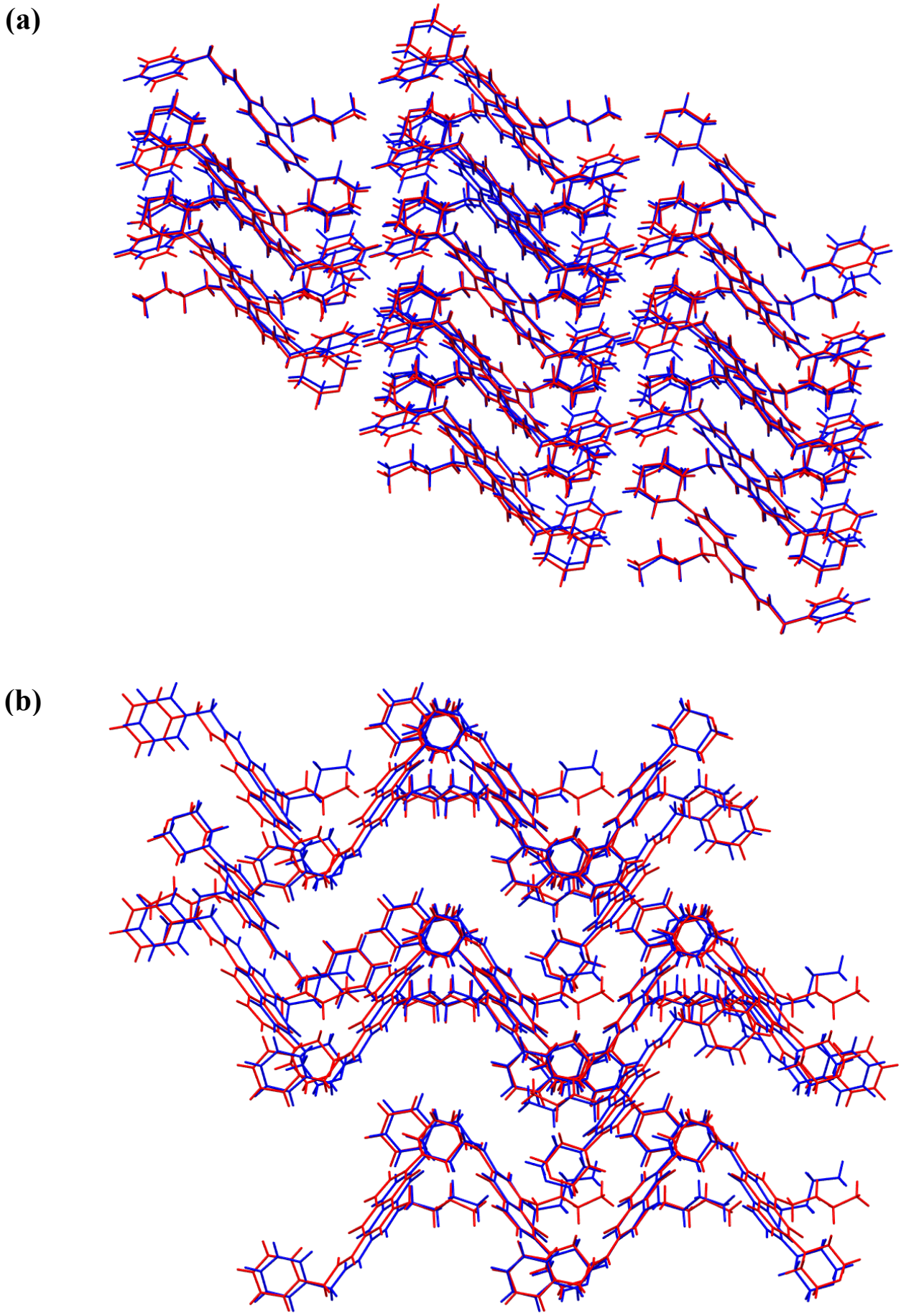

Figure S10: Crystal packing similarity between the HT and LT phases of **(a) Form I** [RMS: 0.305 for HT (red) vs LT (blue)] and **(b) Form II** [RMS: 0.499 for HT (red) vs LT (blue)]. Analysis carried out using a cluster of 30 molecules in *Mercury* 2024.3.1. Each atom's hydrogen and bond counts were ignored due to disordered atoms in the HT structures.

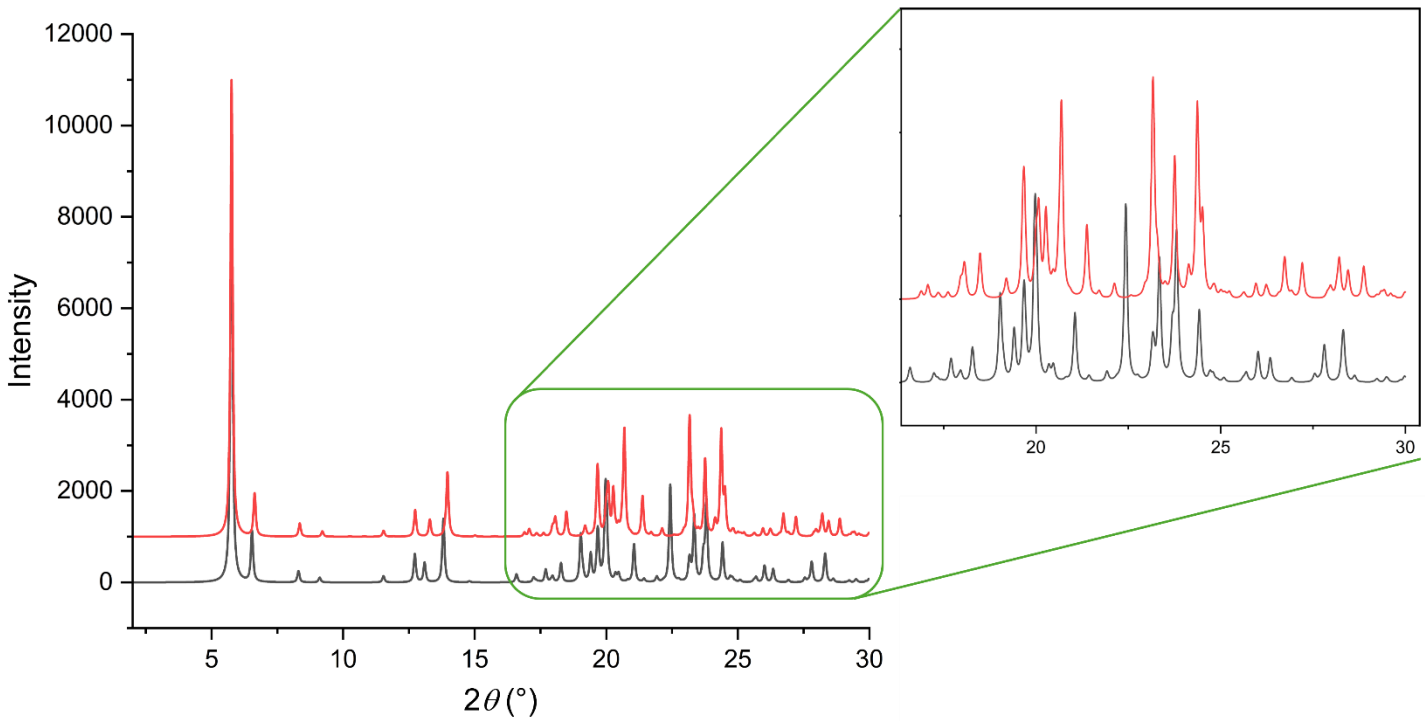

Figure S11: The simulated PXRD patterns of crystal structures of the HT (298 K; black) and LT (100 K; red) phases of **Form I**.

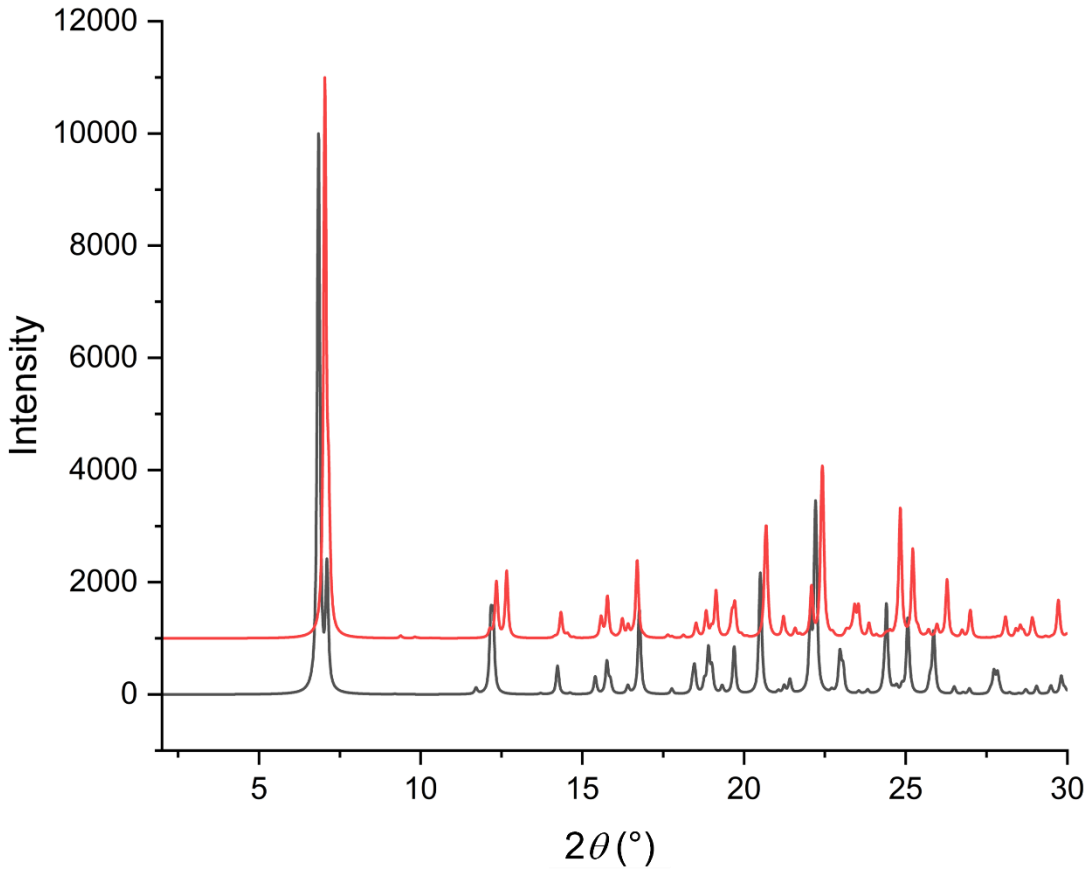

Figure S12: The simulated PXRD patterns of crystal structures of the HT (298 K; black) and LT (100 K; red) phases of **Form II**.

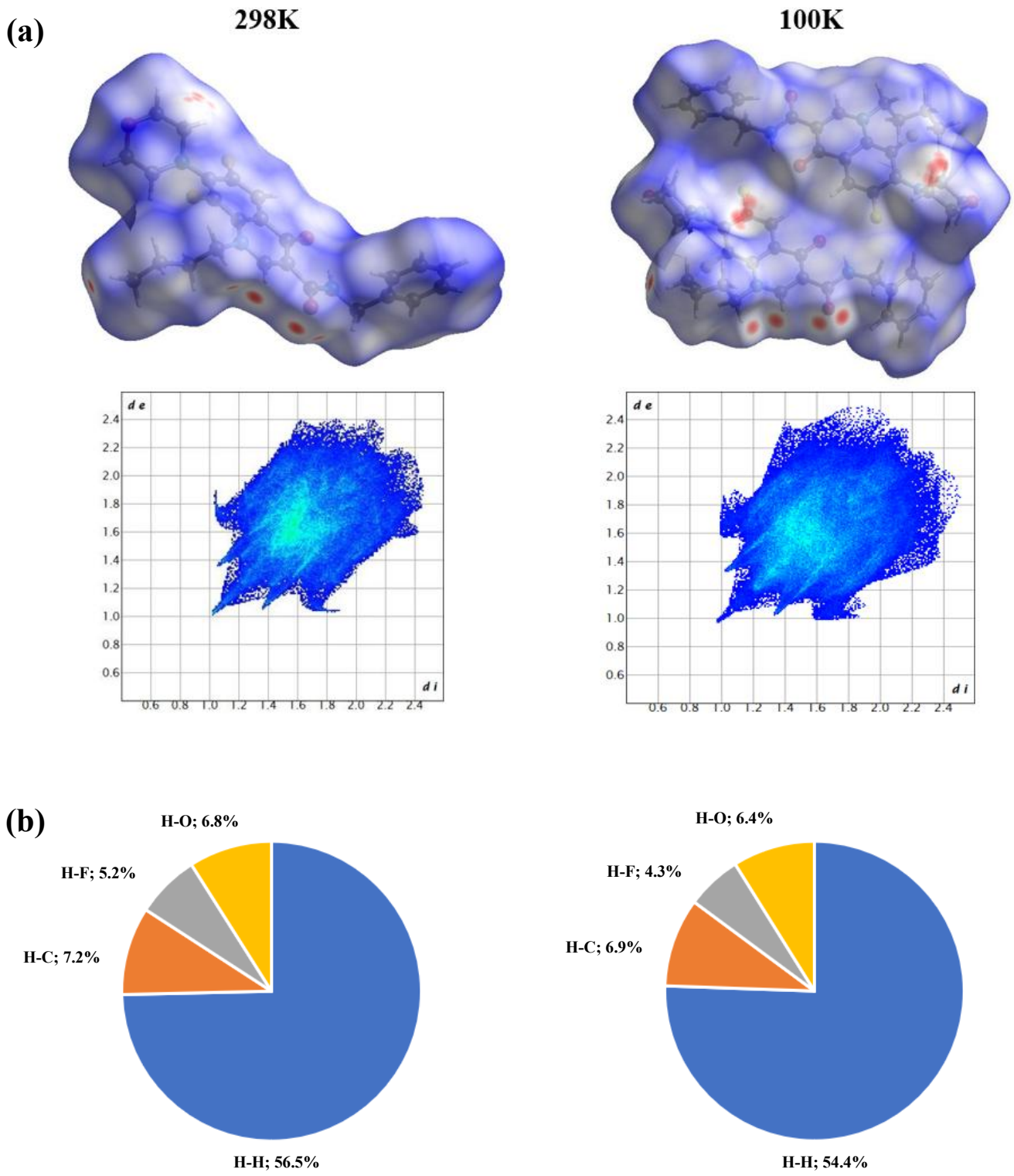

Figure S13: (a) Hirshfield surfaces and the corresponding fingerprint plots depicting the interactions for the major conformer of the HT (298K) and LT (100K) phases of **Form I**. **(b)** Pie-charts depicting the percentage contributions of major interactions in each of the phases.

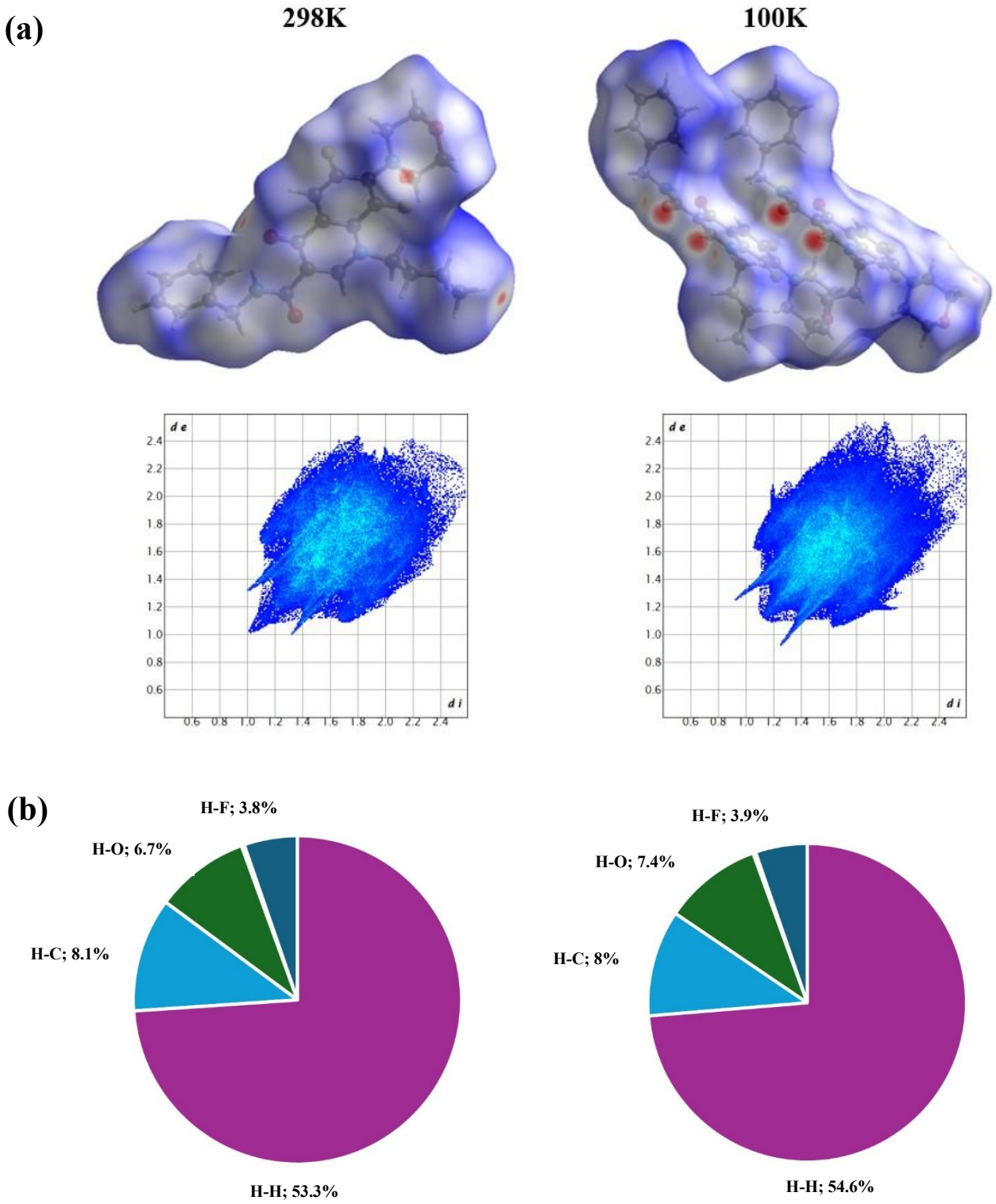

Figure S14: (a) Hirshfield surfaces and the corresponding fingerprint plots depicting the interactions for the major conformer of the HT and LT phases of **Form II**. **(b)** Pie-charts depicting the percentage contributions of major interactions in each of the phases.

Table S14 (a): Pairwise interaction energies calculated at the B3LYP/6-31G(d,p) level of theory for HT Phase (298K) of **Form I**.

Symop	R	E_ele	E_pol	E_dis	E_rep	E_tot
-x, -y, -z	7.37	-13.7	-4.4	-45.2	20.9	-44.2
-x, -y, -z	8.91	-44.1	-14.5	-61.4	55.9	-76.3
-x, -y, -z	16.24	1.3	-0.3	-5.4	0	-3.5
x, y, z	16.13	-0.9	-0.7	-15.3	0	-14.8
x, y, z	15.41	-1.4	-0.1	-5.5	0	-6.3
-x, -y, -z	7.32	-9	-3	-39.1	14.4	-36.8
-x, -y, -z	6.94	-15.6	-4	-50.1	39.5	-38.7
x, y, z	5.45	-13.5	-4.7	-94.6	45.1	-72.2
-x, -y, -z	14.85	1.1	-0.2	-2.5	0	-1.2
-x, -y, -z	16.68	-1.8	-1	-11.6	0	-12.7
x, y, z	18.5	-2.5	-0.2	-3.2	0	-5.6

Table S14 (b): Pairwise interaction energies calculated at the B3LYP/6-31G(d,p) level of theory for LT Phase (100K) of **Form I**.

Symop	R	E_ele	E_pol	E_dis	E_rep	E_tot
-x, y+1/2, -z+1/2	10.57	-0.4	-0.4	-12.1	2.9	-9.5
x, y, z	16.27	0.3	-0.6	-13.6	0	-12
x, y, z	19.38	-0.5	-0.1	-2.4	0	-2.7
x, y, z	6.07	-14.4	-4.5	-95.9	49.9	-71.2
-x, y+1/2, -z+1/2	9.50	-11	-3.5	-35	20.2	-32.2
-x, -y, -z	8.93	-47.5	-15.4	-58.4	53.4	-79.5
x, y, z	15.1	-1.2	-0.1	-4.1	0	-4.9
-x, -y, -z	6.82	-9.6	-4.7	-45.1	16.2	-42.9
-x, y+1/2, -z+1/2	11.93	-5.3	-1.4	-13.1	8	-13.1
-x, -y, -z	16.26	2.1	-0.2	-6.4	0	-3.5

Table S14 (c): Pairwise interaction energies calculated at the B3LYP/6-31G(d,p) level of theory for HT Phase (298K) of **Form II**.

Symop	R	E_ele	E_pol	E_dis	E_rep	E_tot
-	5.24	-21.4	-5.7	-114.1	68.9	-83.8
-x, -y, -z	7.04	-12.7	-3.8	-45.1	21.3	-42.3
x, y, z	18.49	0.7	-0.2	-4.1	0	-2.9
-	16.11	-1.5	-0.9	-18.3	0	-18.2
x, y, z	15.41	-0.6	-0.1	-6.2	0	-6.1
-	5.42	-17.8	-5.6	-104.4	60.4	-76.5
-	6.82	-17.9	-4.6	-56	45.3	-43.2
-	8.82	-49.9	-16.4	-65.6	65.5	-81.6
-	16.22	1	-0.9	-18.6	0	-15.8
-x, -y, -z	7.44	-14.1	-6.4	-40.8	16.9	-44.8
-	16.75	3.1	-1.3	-12.7	0	-8.7
-x, -y, -z	14.84	1.3	-0.2	-3	0	-1.3
-	18.35	-0.4	-0.2	-2.7	0	-2.9
-x, -y, -z	16.41	1.5	-0.2	-3.9	0	-2
-x, -y, -z	6.99	-18.4	-5.7	-56.8	32.4	-53.1
x, y, z	15.41	-0.6	-0.1	-7.7	0	-7.4
-x, -y, -z	14.92	1.7	-0.2	-3.5	0	-1.5
-x, -y, -z	7.58	-9.2	-2.9	-38.5	18.8	-33.8
x, y, z	18.49	-2.5	-0.2	-2.9	0	-5.4
-x, -y, -z	16.04	3.1	-0.3	-6	0	-2.2

Table S14 (d): Pairwise interaction energies calculated at the B3LYP/6-31G(d,p) level of theory for LT Phase (100K) of **Form II**.

Symop	R	E_ele	E_pol	E_dis	E_rep	E_tot
-x, y+1/2, -z+1/2	10.32	-0.5	-0.5	-13.9	4.6	-10.2
-	6.03	-24.2	-5.6	-118.5	76.6	-85.5
-x, y+1/2, -z+1/2	11.83	-6.7	-1.7	-14.5	11.6	-13.8
x, y, z	14.57	-0.9	-0.1	-6.5	0	-6.7
-x, -y, -z	8.83	-50.5	-18.3	-66.8	69.3	-82.3
-	15.76	-6.4	-0.8	-13.9	0	-19.4
-	15.53	1.1	-0.2	-4.8	0	-3.1
-	9.34	-14.5	-3.7	-39.4	27.7	-35.3
-	6.17	-18	-4.9	-102.5	60.6	-74.4
-	9.23	-9.7	-3.6	-34.5	22.5	-29.1
-	6.78	-10.1	-5.3	-47.3	22.3	-42
x, y, z	19	-0.3	-0.2	-4.3	0	-4.1
-	15.83	-0.6	-0.9	-17.4	0	-16.4
x, y, z	14.57	-1.4	-0.1	-4	0	-5
-x, y+1/2, -z+1/2	10.42	-0.9	-0.4	-13.4	5.6	-9.4
-x, -y, -z	8.86	-55.2	-17.6	-69.6	74.5	-85.9
x, y, z	19	-1.5	-0.1	-3.1	0	-4.4
-x, -y, -z	17.48	-0.3	-0.2	-3.6	0	-3.6
-x, y+1/2, -z+1/2	11.77	-5.6	-1.6	-14.5	10.8	-13.1

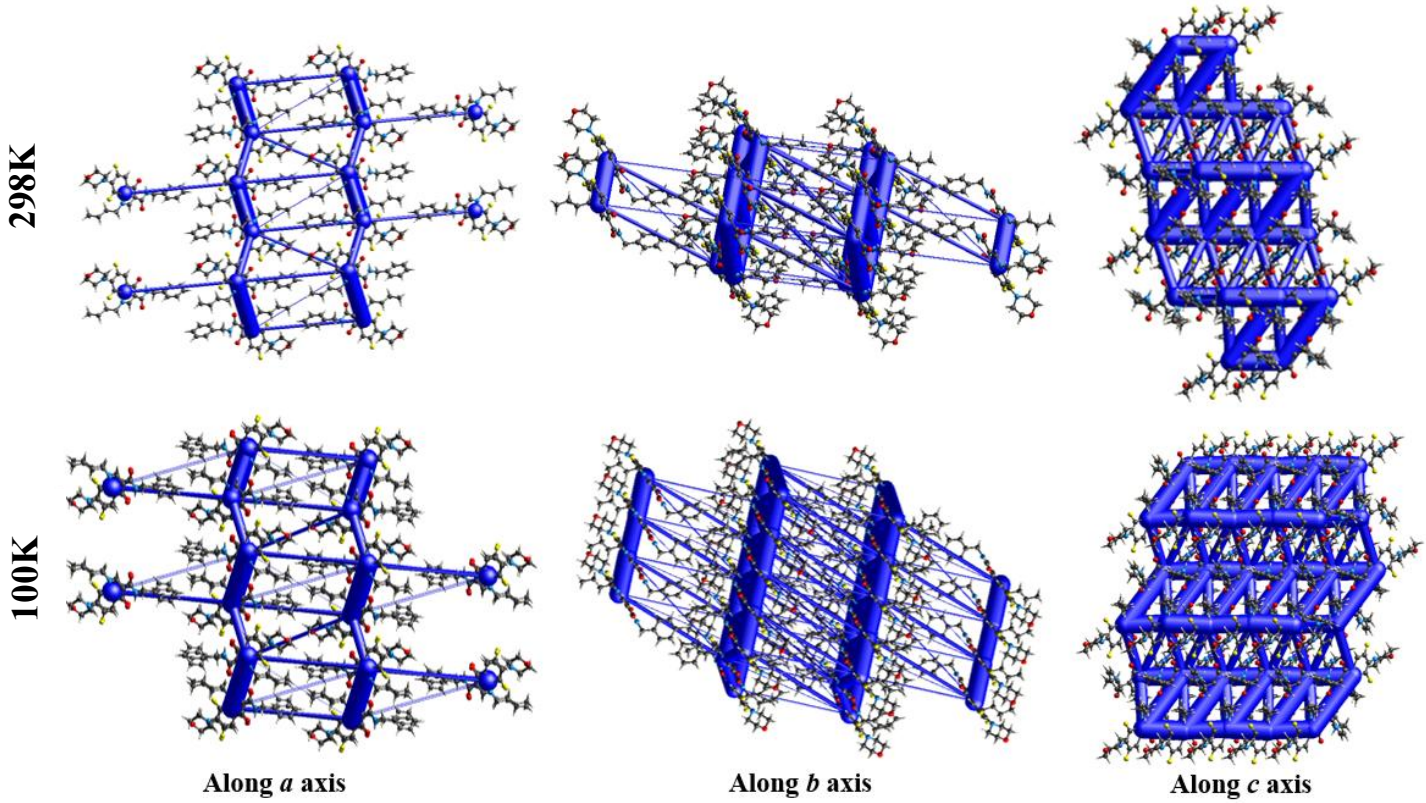

Figure S15: *CrystalExplorer*-based energy frameworks in terms of the total energies for the crystal structures of the major conformer of the HT phase (298K) and the LT phase (100K) of **Form I**.

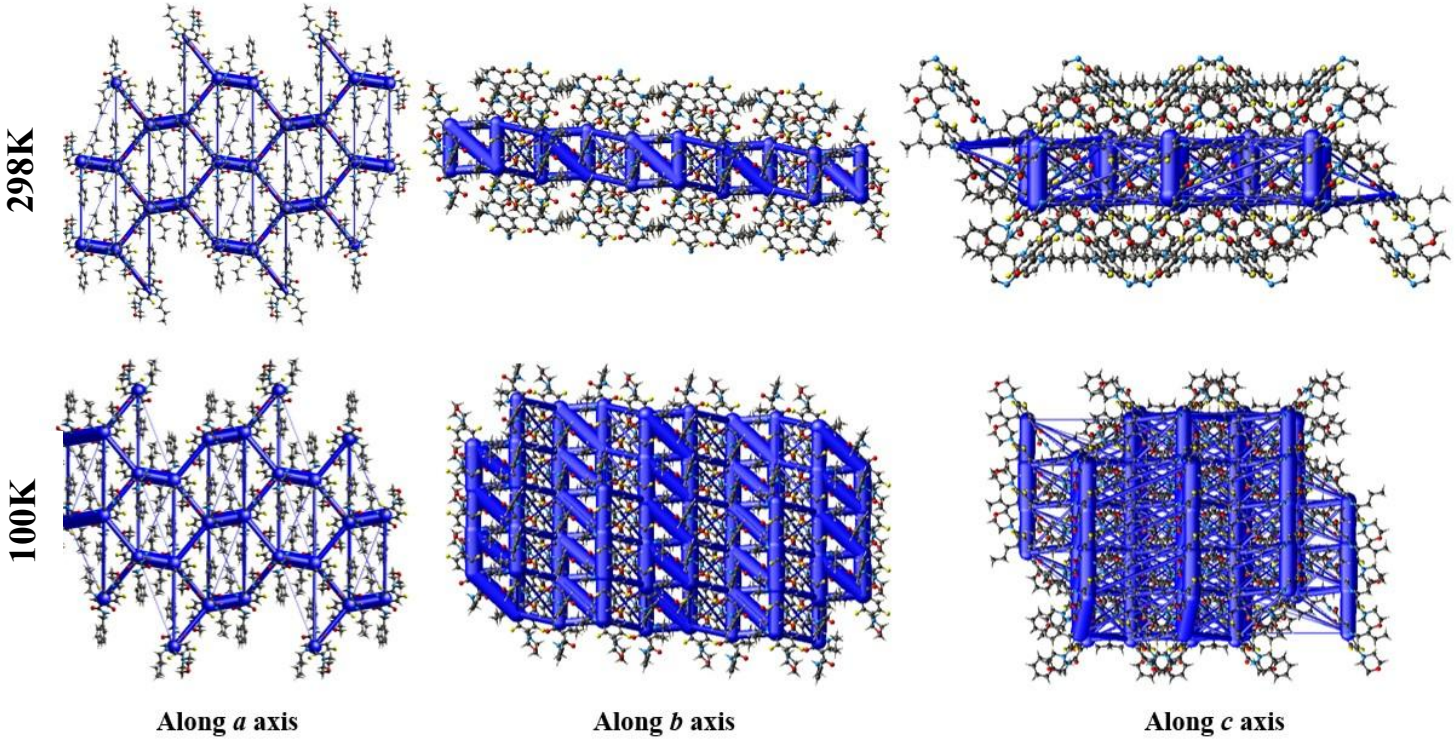

Figure S16: *CrystalExplorer*-based energy frameworks in terms of the total energies for the crystal structures of the major conformer of the HT phase (298K) and the LT phase (100K) of **Form II**.

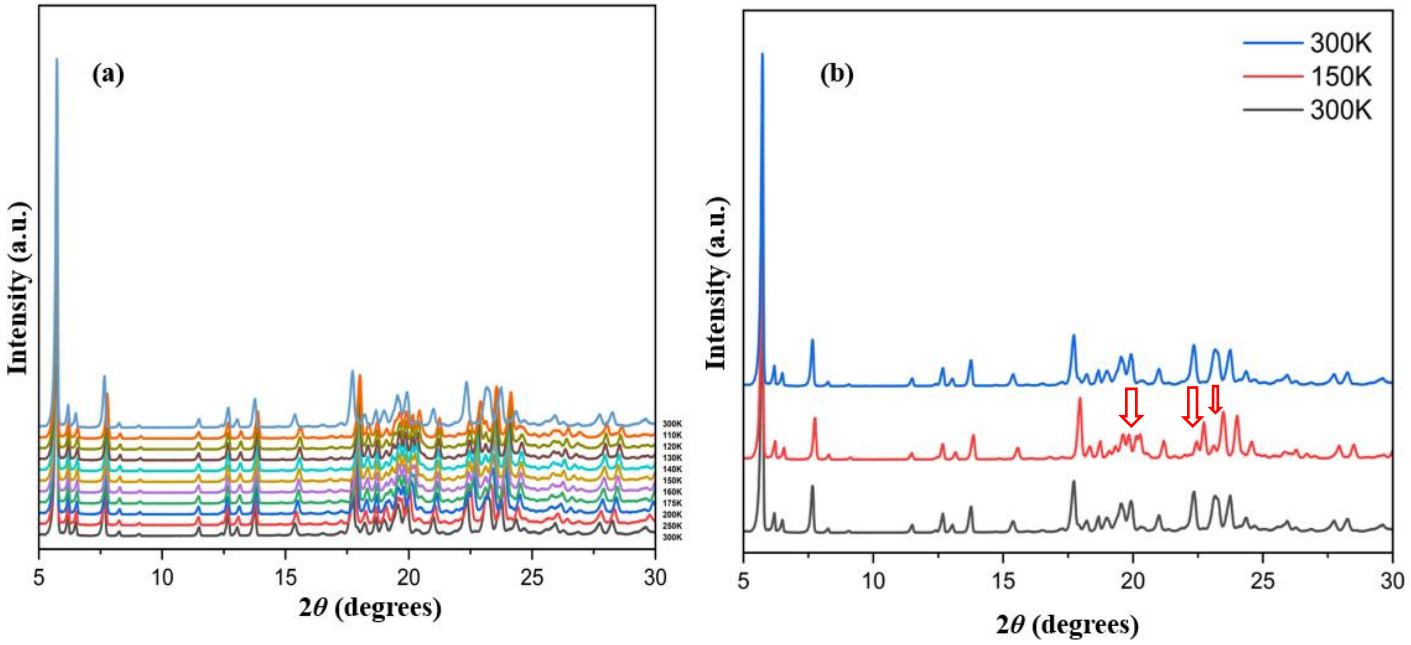

Figure S17: **(a)** Stacked PXRD patterns of **Form I** for the cooling cycle from 300K to 110K and 300K in the heating cycle (light blue). **(b)** Stacked PXRD patterns of **Form I** to demonstrate the reversibility of the phase transition.

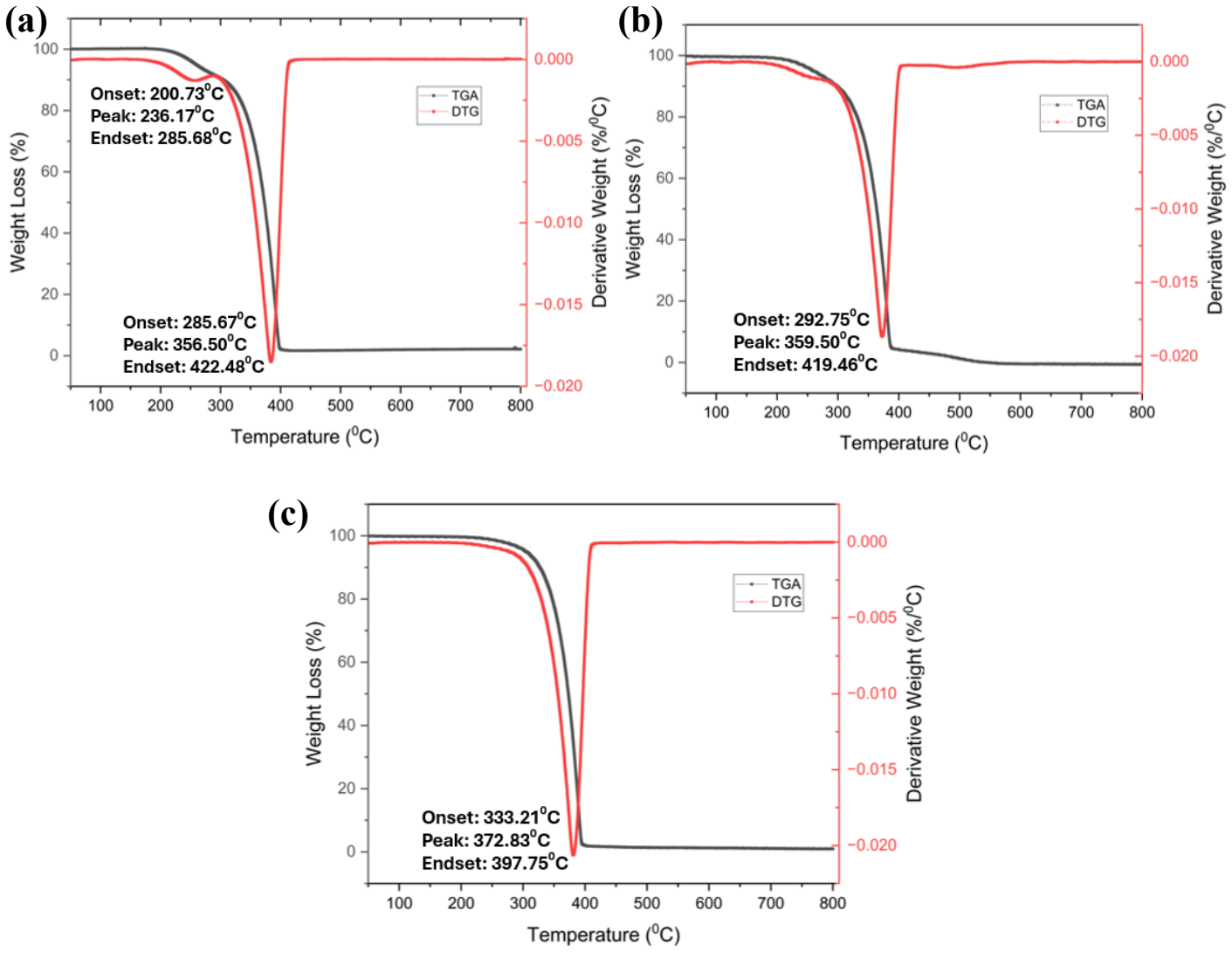

Figure S18: TGA and DTG thermograms recorded for **(a) 1**, **(b) Form I**, and **(c) Form II.**

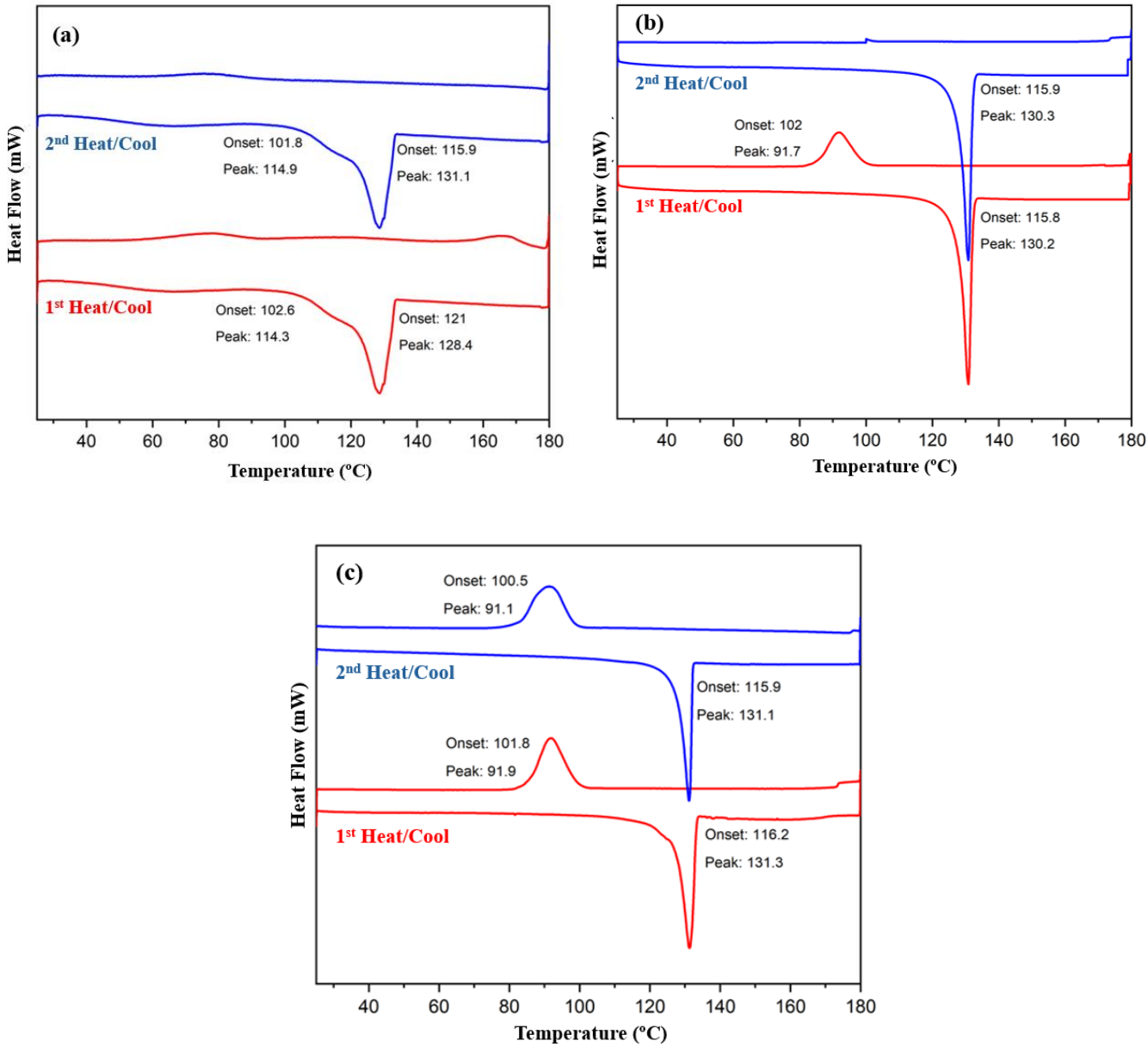

Figure S19: DSC thermograms in the range 35-180ºC recorded for **(a) 1**, **(b) Form I**, and **(c) Form II.**

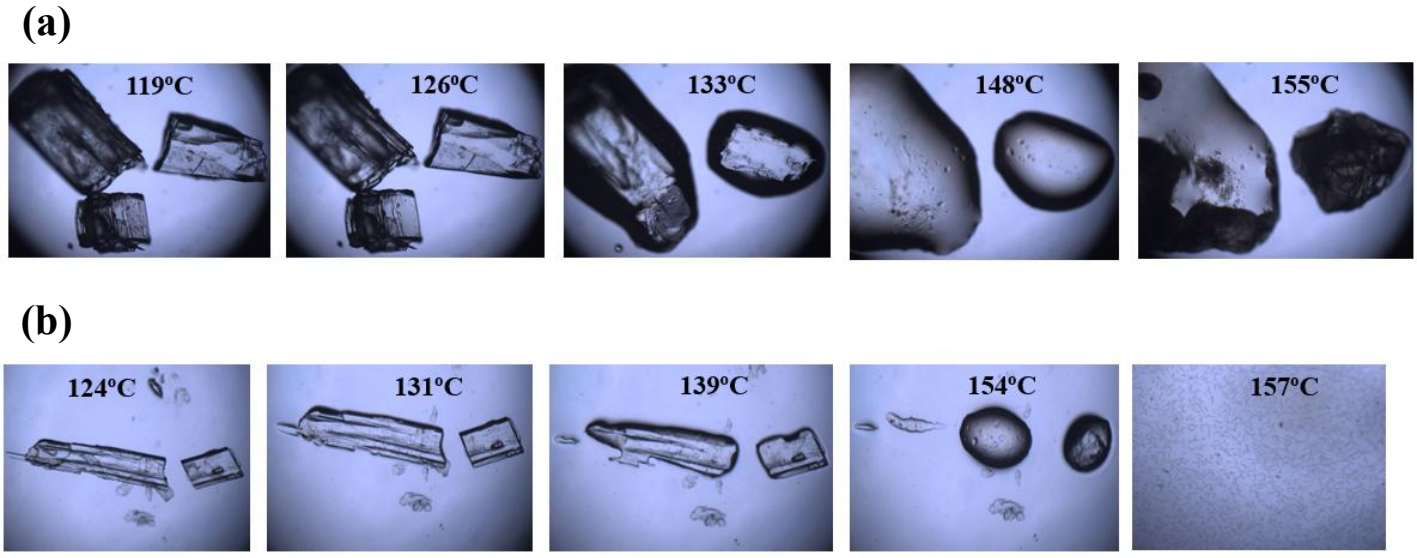

Figure S20: HSM images captured at various temperatures for **(a) Form I** and **(b) Form II**.

Table S15: CTE (α) in MK^{-1}, their standard deviation (σ_α), and directions of **Form I**.

HT Phase (298-160K)					
Axes	**α(MK^{-1})**	**σ_α(MK^{-1})**	***a***	***b***	***c***
X1	**-17.9**	7.5	0.8130	0.3177	0.4880
X2	55.1	3.7	0.7218	0.6035	-0.3388
X3	150.3	3.9	0.9766	-0.1967	-0.0870
V	189.2	5.7			
LT Phase (150-100K)					
Axes	**α(MK^{-1})**	**σ_α(MK^{-1})**	***a***	***b***	***c***
X1	145.4	4.9	0.8348	-0.5268	0.1600
X2	12.9	6.5	-0.2477	0.1439	0.9581
X3	**-52.1**	11.6	0.6728	-0.7362	-0.0729
V	106.8	18.9			

Table S16: CTE (α) in MK^{-1}, their standard deviation (σ_α), and directions of **Form II**.

HT Phase (298-180K)					
Axes	**α(MK^{-1})**	**σ_α(MK^{-1})**	***a***	***b***	***c***
X1	231.3	9.5	0.9113	0.0	0.4118
X2	10.5	8.5	0.9932	0.0	-0.1166
X3	**-75.7**	9.4	0.0000	1.0	0.0000
V	167.3	26.1			
LT Phase (170-100K)					
Axes	**α(MK^{-1})**	**σ_α(MK^{-1})**	***a***	***b***	***c***
X1	34.9	5.0	0.0000	1.0	0.0000
X2	67.0	4.7	0.9513	0.0	0.3083
X3	15.7	6.7	0.7823	0.0	-0.6229
V	117.2	11.5			

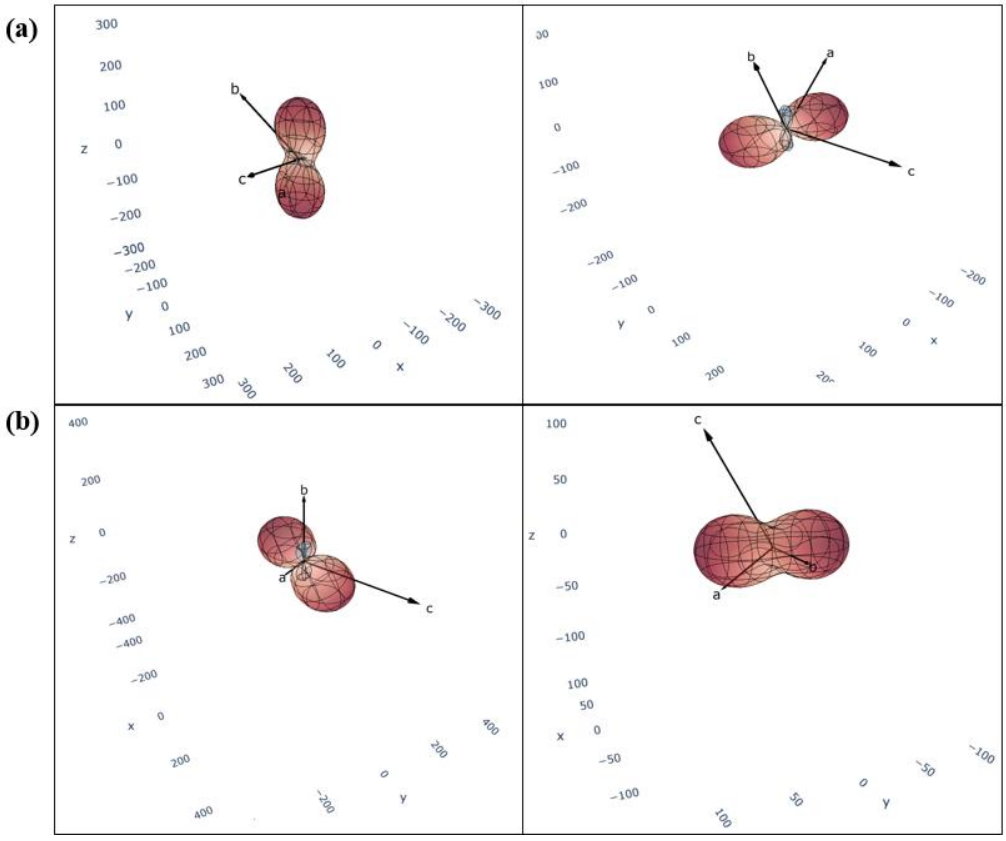

Figure S21: Thermal expansivity indicatrix plots depicting PTE and NTE effects in the HT (left) and LT (right) phases of **(a) Form I** and **(b) Form II**.

(a)

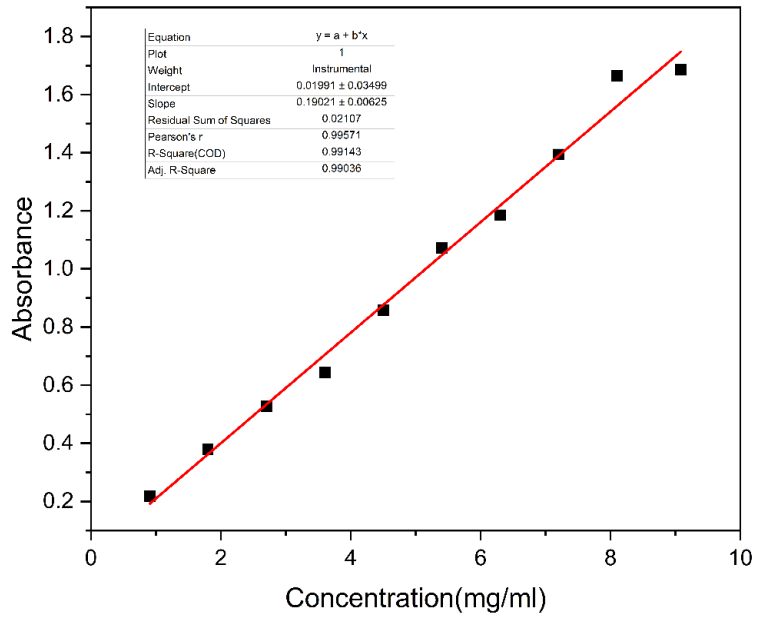

(b)

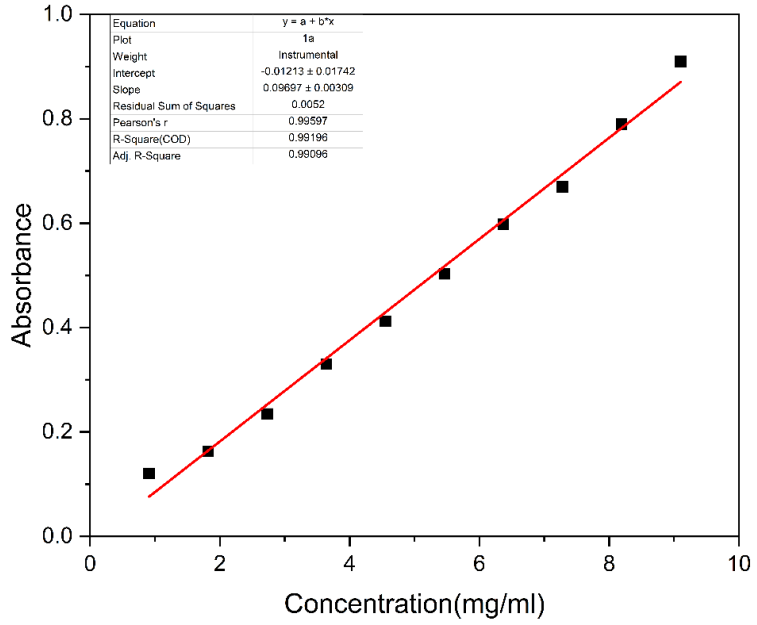

(c)

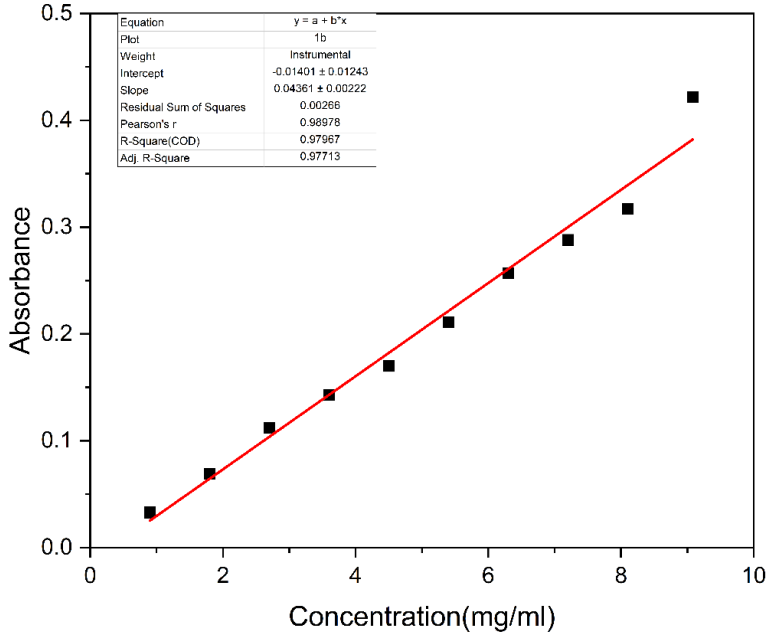

Figure S22: Calibration plots of the equilibrium solubility analysis of **(a) 1**, **(b) Form I,** and **(c) Form II**.

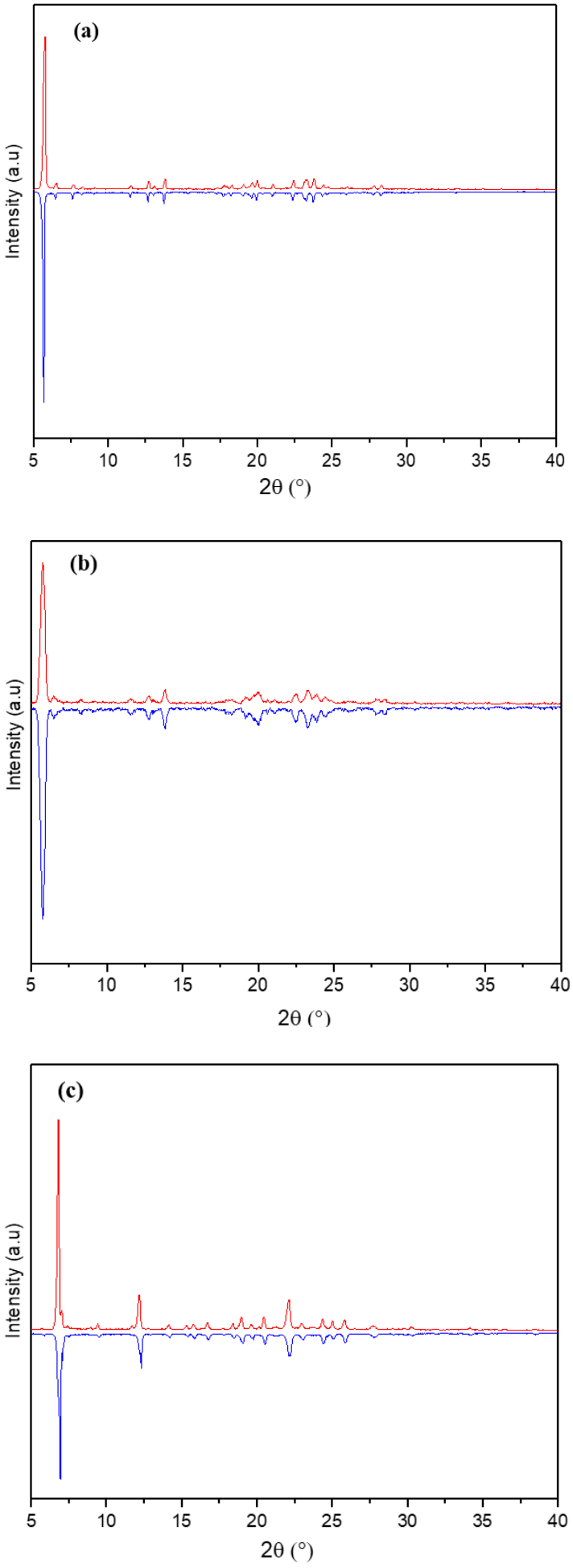

Figure S23: Experimental PXRD patterns of **(a) 1**, **(b) Form I**, and **(c) Form II** before (in red) and after (in blue) dissolution to demonstrate phase stability.